Biochimica et Biophysica Acta (BBA) - General Subjects (3226-3237)
1840(11):2014.9.

Scavenger receptor CL-P1 mediates endocytosis by associating with AP-2 μ 2.

Jang S, Ohtani K, Fukuoh A, Mori K, Yoshizaki T, Kitamoto N, Kim Y, Suzuki Y, Wakamiya N.

SCAVENGER RECEPTOR CL-P1 MEDIATES ENDOCYTOSIS BY ASSOCIATING WITH AP-2 μ2*

SeongJae Jang[a,1], Katsuki Ohtani[a,1], Atsushi Fukuoh[a], Kenichiro Mori[a], Takayuki Yoshizaki[a], Noritoshi Kitamoto[b], YounUck Kim[a], Yasuhiko Suzuki[c], Nobutaka Wakamiya[a,*]

[a]Department of Microbiology & Immunochemistry, Asahikawa Medical University, 2-1-1-1 Midorigaoka-Higashi, Asahikawa 078-8510, Japan

[b]Department of Microbiology, School of Human Science and Environment, University of Hyogo, Himeji 670-0092, Japan

[c]Department of Bioresources, Research Center for Zoonosis Control, Hokkaido University, Sapporo 001-0020, Japan

Running head: CL-P1 utilizes AP-2 μ2 in endocytosis

[1]The first two authors contributed equally to this work.

*to whom correspondence should be addressed: Dept. of Microbiology and Immunochemistry, Asahikawa Medical University, 2-1-1-1 Midorigaoka-Higashi, Asahikawa 078-8510 Japan. Tel:81-166-68-2393; Fax:81-166-68-2399; E-mail address: wakamiya@asahikawa-med.ac.jp

Keywords: Scavenger Receptors, Endocytosis, Adaptor complex, Collectin, Tyrosine motif

ABSTRACT

Background: Scavenger receptor CL-P1 (collectin placenta 1) has been found recently as a first membrane-type collectin which is mainly expressed in vascular endothelial cells. CL-P1 can endocytose OxLDL as well as microbes but in general, the endocytosis mechanism of a scavenger receptor is not well elucidated.

Methods: We screened a placental cDNA library using a yeast two-hybrid system to detect molecules associated with the cytoplasmic domain of CL-P1. We analyzed the binding and endocytosis of several ligands in CL-P1 transfectants and performed the inhibition study using tyrphostin A23 which is a specific inhibitor of tyrosine kinase, especially in μ2-dependent endocytosis and the site-directed mutagenesis in the endocytosis YXXΦ motif in CL-P1 cytoplasmic region. Furthermore, the SiRNA study of clathrin, adaptor AP-2 and dynamin-2 during the endocytosis of OxLDL in CL-P1 transfectant cells were carried out.

Results: We identified μ2 subunit of the AP-2 adaptor complex as a molecule associated with the cytoplasmic region of CL-P1. We demonstrated that AP-2 μ2 was essential for CL-P1 mediated endocytosis of OxLDL in CL-P1 transfectant cells and its endocytosis was also mediated by clathrin, dynamin and adaptin complex molecules.

Conclusions: Tyrosine-based YXXΦ sequences play an important role in CL-P1-mediated OxLDL endocytosis associated with AP-2 μ2.

General Significance: This might be the first finding of the clear endocytosis mechanism in scavenger receptor CL-P1.

1. Introduction

The scavenger receptor family is a highly heterogenous group of cell surface molecules that commonly bind and uptake modified low density lipoproteins (LDLs), such as acetylated LDL (AcLDL) and oxidized LDL (OxLDL). OxLDLs are considered to be most active in interactions among endothelial cells (EC), macrophages, and smooth muscle cells, and have been implicated in the development of atherosclerosis according to Ross's response-to-injury hypothesis (1, 2). The scavenger receptor family has at least eight different subclasses (Class A - Class H) which bear little sequence homology to each other but recognize common ligands (3). Vascular endothelial cells express several distinct scavenger receptors, such as SR-BI (4-6), LOX-1 (7), SREC (8), FEEL-1/stabilin-1 and FEEL-2/stabilin-2 (9).

We recently identified collectin placenta 1 (CL-P1) from placental cDNA, which is a C-type lectin containing an inner collagen-like region (10). CL-P1 is a type II transmembrane protein with a coiled-coil domain, a collagen-like domain, and a carbohydrate recognition domain (CRD). It resembles Class A scavenger receptors (SR-A) in that the scavenger receptor cysteine-rich domain is replaced by a CRD (11). The ability of CL-P1 to bind and phagocytose Gram-negative and Gram-positive bacteria, as well as to yeast, strongly suggests a role for CL-P1 in host defense. Recently, we demonstrated an important role of scavenger receptor CL-P1 in zymosan phagocytosis by several vascular endothelial cells (12).

Interestingly, CL-P1 can also bind and endocytose OxLDL but not to AcLDL as other modified-LDLs in endothelial cells (10). LOX-1 is a class E scavenger receptor that was originally considered as the major and only receptor for OxLDL on endothelial cells (7). Arterial CL-P1 was upregulated in the endothelium after the induction of oxidative stress in vitro as well as in a rat ischemia-reperfusion model (13). In this report, CL-P1 exhibited a different temporal profile than LOX-1 in that it appeared later in vascular endothelial cells in rat (13). Furthermore, it showed that the endothelium having CL-P1 overexpressed due to the oxidative stress in rat could endocytose OxLDL there (13).

Clathrin triskelions and the clathrin adaptor complex AP-2 are the major components of the clathrin coats located at the plasma membrane, and are responsible for the endocytosis of various proteins, lipids, and viral particles (14). Recently, LOX-1 was reported to be internalized by a clathrin-independent and dynamin-2-dependent pathway and was thus thought likely to mediate OxLDL trafficking in vascular tissues (15). Although CL-P1 and Lox-1 might have performed some role as scavenger receptors in vascular endothelial cells, but definitive mechanisms or related molecules related with CL-P1 endocytosis are not elucidated. In our current study, we demonstrated that scavenger receptor CL-P1 bound directly to AP-2 μ2 in receptor–mediated endocytosis through a tyrosine-motif-dependent pathway.

2. Materials and methods

2.1. Reagents and Antibodies

Ham's F12 medium was obtained from Sigma-Aldrich (Poole, UK). Fetal bovine serum was obtained from Invitrogen Co. (Carlsbad, CA). Alexa Fluor 488-and Alexa Fluor 594-conjugated anti-rabbit, anti-mouse IgG antibody, and Hoechst 33342 were from Invitrogen Co. (Molecular Probes, Eugene, OR). Wortmannin, tyrphostin A23 and genistein were from Calbiochem (San Diego, CA). Monoclonal antibody to β-actin (AC-74) was from Sigma-Aldrich (Poole, UK). Monoclonal antibody to clathrin heavy chain, α-adaptin, β-adaptin, μ2 (AP50) and dynamin-2 were purchased from BD Biosciences (San Jose, CA). Monoclonal and polyclonal antibodies to CL-P1 (10, 12) were obtained using the recombinant carbohydrate recognition domain (CRD) of human CL-P1 in *E. coli*. Immunoaffinity purification of antibodies was used to purify antigen-specific antibodies from a preparation of polyclonal antibodies to CL-P1. All restriction enzymes were from New England Biolabs (Ipswich, MA).

2.2. Yeast two-hybrid screening

The *Saccharomyces cerevisiae* strain AH109 was maintained on YPD agar plates. Transformation was carried out using the lithium acetate procedure described in the instructions for the MATCHMAKER two-hybrid kit (Takara Bio). An adult human placental cDNA library (Takara Bio) was directly cloned into pGADT7 as an in-frame fusion with Gal4 AD. This library was co-transformed with the pGBKT7/CL-P1NT construct as a bait into the yeast strain AH109, with the integrated growth selection reporter gene *HIS3* using the polyethylene glycol/lithium acetate procedure. Positive clones were isolated by growth on histidine–free medium. After 5 days at 30°C, their ability to grow on plates lacking histidine and the level of β-galactosidase (X-α-gal) activity were tested. To examine direct interaction, the yeast stain AH109 was co-transformed with the indicated constructs and analyzed by growth in selective medium lacking histidine. In the liquid β-galactosidase assay, cultures of transformants were prepared according to the instructions supplied with the MATCHMAKER two-hybrid kit. β-galactosidase activity was measured using a chemiluminescent β-galactosidase assay kit (Takara Bio) and a luminometer. Briefly, yeast cells were resuspended at 10 A_{600}/ml in lysis buffer and disrupted by vortexing in the presence of glass beads. After centrifugation at 4°C for 15 min in a microcentrifuge, 10-50 μl of the lysate were used for the measurements. Results were normalized by the protein concentration and expressed as the mean ± standard deviation of three independent determinations.

2.3. Plasmids and their construction

The GAL4 DNA-binding domain constructs (GAL4BD)-CL-P1NT/Wild, GAL4BD-CL-P1NT/E7,8A, GAL4BD-CL-P1NT/E9,10A, GAL4BD-CL-P1NT/S13A, GAL4BD-CL-P1NT/Y16A and

GAL4BD-CL-P1NT/F19A, were formed by ligation of polymerase chain reaction fragments into *BamH* I and *Not* I sites of the vector pGBKT7 (Takara Bio). Constructs having GAL4AD-fused μ1, μ3, μ4, μ2 (1-453), μ2 (1-141), and μ2 (142-453) were formed by ligation of polymerase-chain reaction-amplified cDNA into the vector pGADT7 (Takara Bio). The GST fusion construct pGEX4T-2/CL-P1NT, was formed by ligation of the CL-P1 cytoplasmic domain (CL-P1NT) cDNA (120-bp) into *BamH* I and *Not* I restriction sites of the vector pGEX4T-2 (GE healthcare). Single or double amino acid substitution with alanine in CL-P1NT was carried out using a QuickChange site-directed mutagenesis kit (Stratagene, La Jolla, CA). Briefly, 50 ng of pGBKT7 plasmids carrying CL-P1NT cDNA were incubated with two complementary primers (2 μM each) containing the desired mutation in the presence of a 2 mM dNTP mixture and 2.5 units of *Pfu* DNA polymerase according to the following protocol: 18 cycles of 0.5 min at 95°C, 1 min at 60°C, and 1 min at 68°C. After replication of both vector strands, the methylated parental DNA was digested for 1 h at 37°C with 10 units of *Dpn I* endonuclease and the nicked vector having the desired mutation was transformed into *E. coli*. All constructs of CL-P1 mammalian expression vectors were assembled using cDNA of wild type human CL-P1; N-terminal amino-acid-substituted mutants inserted into the expression vector pcDNA 3.1/myc-His A have been described previously (10, 12).

2.4. *GST pull-down Assays*

The expression vectors for glutathione S-transferase fusion proteins pGEX4T-2 (GST) and pGEX4T-2/CL-P1NT (GST-CL-P1NT) were introduced into the BL21 strain of *Escherichia coli*. The bacterial cultures were induced by isopropyl-1-thio-β-D-galactoside (IPTG) at a final concentration of 0.1 mM for 5 h at 37°C. *E. coli* were pelleted and washed with the STE buffer (10 mM Tris-HCl pH 7.4, 150 mM NaCl, 1 mM EDTA) and incubated with STE buffer containing 100 μg of lysozyme (Sigma-Aldrich) for 15 min on ice. Protease inhibitor cocktails (Roche Diagnostics, Mannheim, Germany) were added to the resuspended *E. coli*, which were then sonicated. Bacterial lysates in 4% Triton X-100, 10 μg of DNase, and 8 mM of $MgCl_2$ were incubated for 2 h at 4°C followed by centrifugation at 10,000 × g for 20 min. GST fusion proteins were purified by binding to glutathione (GSH)-Sepharose 4B beads (GE healthcare) at room temperature for 1 h followed by washing three times with phosphate-buffered saline containing protease inhibitors, and were then eluted with an elution buffer (50 mM Tris-HCl, pH 9.6, 150 mM NaCl, 10 mM glutathione). The purified GST fusion proteins were dialyzed against PBS containing 2 mM EDTA and 1 mM dithiothreitol. ^{35}S-labeled medium chains of adaptor complexes (μ1, μ2, μ3, and μ4) and truncated mutants of μ2 were assembled by *in vitro* transcription and translation from a T7 promoter using a TNT T7 Quick Coupled Transcription/Translation System (Promega), according to the supplier's protocol. Prior to pull-down experiments, aliquots of TNT reactions were electrophoresed and the amounts of labeled medium chains were

determined by phosphor-imaging. The GST-CL-P1NT fusion protein was incubated with the ^{35}S-labeled medium chains of adaptor complexes or luciferase translation products at 4°C for 2 h in 0.5 ml of binding buffer (50 mM HEPES-KOH pH 7.4, containing 150 mM KCl, 10 mM $MgCl_2$, 10 % (v/v) glycerol, 1 % (v/v) Triton X-100, and 0.2 % bovine serum albumin) followed by the addition of 50 μl (50 % v/v) glutathione-agarose in binding buffer for a further 2 h at 4°C. The beads were washed four times with binding buffer without bovine serum albumin. The bound proteins were extracted by boiling for 5 min in SDS-sample buffer containing β-mercaptoethanol and separated by SDS-PAGE (10 % to 20 % gradient polyacrylamide gel). The gels were then exposed to a BAS-MS Imaging Plate.

2.5. Ligand Binding and Endocytosis Assays

We used the permanent transfectant and transient transfectant cells (CHO/CL-P1) which was transfected with the full-length human CL-P1 cDNA containing a *myc*-tag at the C-terminus or empty vector into CHO-ldlA7 (lacking functional LDL receptors). For immunofluorescence studies, Alexa Fluor 488-labeled antibodies of CL-P1 (5 μg/ml in culture medium supplemented with 0.2% BSA) were applied to cells grown on a glass-bottomed dish and incubated for 30 min on ice. For quantitative uptake assays, biotinylated antibodies of CL-P1 were added to 35 mm wells. Unbound ligand was removed by several quick washes with pre-warmed serum free medium, and the bound ligand was incubated at 37°C for varies lengths of time in 0.2% BSA-containing medium to allow for internalization. Internalized biotinylated CL-P1 antibodies were quantitated by western blotting using streptavidin-conjugated to horseradish peroxidase (GE Healthcare). Signals were detected using enhanced chemiluminescence (ECL Plus, GE Healthcare). The results were visualized using an LAS-3000 Lumino-Image Analyzer (GE Healthcare). For quantitative analysis, internalized fluorescence-labeled mAb were measured as fluorescence values after quenching treatment by Twinkle LB 970 Microplate Fluorometer (BERTHOLD TECHNOLOGIES, GmbH & Co. KG).
For inhibition experiments, cells were preincubated with wortmannin (200 nM), tyrphostin A23 (3.5 ~ 350 μM) and genistein (100 μM) for 1h at 37°C prior to the addition of ligand. All experiments were independently performed at least three times, and data are expressed as means ± s.e.m.

2.6. Lipoprotein isolation, modification, and labeling

LDL (d=1.019 to 1.063 g/mL) was isolated by sequential ultracentrifugation of fasting plasma from healthy volunteers using EDTA as the anticoagulant. LDL was oxidized by incubating 0.2 mg/mL LDL in PBS that contained 5 μmol/L $CuSO_4$, at 37°C for 3, 6, 10, or 24 h as previously described (10). Fluorescent labeling of LDL was performed by adding 10 μL of 30 mg/mL 1,1'-dioctadecyl-3,3,3',3'-tetramethylindocarbocyanine

perchlorate (DiI) in dimethyl sulfoxide to 1 mg (protein) of oxidized LDL. The mixture was incubated under sterile conditions at 37°C for 18 hrs. Labeled lipoproteins were isolated by ultracentrifugation (2 cycles of 100,000xg for 20 min). This procedure typically resulted in incorporation of 5-15 μg of DiI per milligram of LDL protein.

2.7. Immunoblotting and lectin blotting

For western blot analysis, CL-P1 cDNA transfected cells, empty vector transfected cells, and siRNA-transfected cells were directly solubilized in SDS-PAGE sample buffer and boiled for 5 min at 95°C. Samples were subjected to SDS-PAGE under reducing conditions and transferred to Immobilon-P (Millipore Corp.). The membranes were blocked for 1 h at room temperature in BlockAce (blocking reagent, DS Pharma Biomedical Co.), and probed with mouse anti-human CL-P1 mAb or other antibodies for 1 h at room temperature. Blots were then washed in 0.1 % Tween 20 in TBS, incubated with secondary antibody conjugated to HRP at a 1:5,000 dilution in washing buffer for 1 h, then washed 3 times. Blots were exposed using an ECL Plus Western Blotting Detection System (GE Healthcare) and analyzed using an LAS-3000 Lumino-Image Analyzer (GE Healthcare).

2.8. Potassium depletion and hypertonic treatment

Potassium depletion was performed according to the method of Larkin *at al.* (16). For potassium depletion, cells were washed with K^+-free buffer (20 mM HEPES pH 7.4, 140 mM NaCl, 1 mM $CaCl_2$, 1 mM $MgCl_2$, 1 mg/ml D-glucose), incubated with hypotonic buffer (K^+-free buffer diluted 1:1 with water) for 5 minutes at 37°C, washed three times with K^+-free buffer and incubated with K^+-free buffer for 30 minutes at 37°C. Cells were incubated with 10 μg/ml DiI-labeled OxLDL and FITC-conjugated Concanavalin A (Sigma) for 1 h at 4°C followed by an endocytic reaction for 1 h at 37°C in K^+-free buffer. Control cells were assayed in the same buffers containing 10 mM KCl. For the hypertonic treatment (17), cells were incubated with complete medium containing 0.45 M sucrose for 15 minutes at 37°C and then incubated with 20 μg/ml DiI-labeled OxLDL for 1 h at 4°C, followed by an endocytic reaction for 1 h at 37°C in complete media with 0.45 M sucrose. Control incubations were carried out in complete medium. Cells were then fixed and processed for immunofluorescence microscopy.

2.9. Immunofluorescence microscopy

Usually, cells were incubated with 10 or 20μg/ml DiI-labeled OxLDL, un-labeled OxLDL for 1 h at 4°C

followed by an endocytic reaction for 1 h at 37°C in several buffers. After these treatments, cells were fixed in 4 % (w/v) paraformaldehyde in PBS and quenched with 50 mM ammonium chloride in PBS. Where stated, cells were permeabilized with 0.1 % Triton X-100 in PBS for 5 min. All subsequent incubations were carried out in 25% (v/v) BlockAce (DS Pharma Biomedical Co.) in PBS. Samples were incubated with FITC-ConA (green) as a cell-surface marker, Hoechst 33342 (blue) (Sigma) as a nuclear marker, sheep-anti-human ApoB antibody (THE BINDINGSITE) followed by Alexa 594 (red) conjugated Donkey anti-sheep IgG in PBS containing 1 mM $CaCl_2$ for 10 min at 4°C immediately before fixation. Cells were then fixed and processed for immunofluorescence microscopy. Coverslips were mounted in SlowFade Gold antifade reagent (Invitrogen). The fluorescent images were observed under an Olympus FLUOVIEW 1000 confocal laser microscope and analyzed using ASW software (version 3.1) or BZ-H1C program (KEYENCE).

2.10. Statistical Analysis

Data are presented as means ± s.e.m. of the specified number of experiments performed in triplicate. The significance of difference was determined by a paired or unpaired Student's *t* test. Unless otherwise stated, data are not significantly different from control values.

3. Results

3.1. CL-P1 interacts with μ2 in a yeast two-hybrid analysis

Multiple sequence alignment of the CL-P1 cytoplasmic domain from mammalian and fish species revealed the conserved sequences of YKRF at residues 16-19 that bear homology to previously characterized endocytic motifs in transferrin (Fig. 1A, 2B). The N-terminal cytoplasmic tail of CL-P1 (CL-P1NT) was used here as bait to screen a human placental cDNA library in a yeast two hybrid assay. The screening of ~ 2 $\times 10^6$ clones yielded a 1.9-kbp cDNA fragment containing a 1,308-bp open reading frame. Sequence similarity searches revealed it to be identical to human μ2, the medium chain of clathrin-associated coated pit adaptor protein complex AP-2. In Figure 1B, yeast two hybrid analysis revealed that AP-2 μ2 interacts with the cytoplasmic domain of CL-P1 (CL-P1NT). We examined the interactions with the four kinds of adaptor medium chain and the cytoplasmic domain of CL-P1 using a GST pull-down assay, and found that only the AP-2 μ2 subunit could bind to GST-CL-P1NT (Fig. 2A). These observations suggest that the fragment of CL-P1 containing the endocytic motif interacts with the μ2 chain of adaptor complexes.

The truncated CL-P1 mutants were used to quantify the interaction between μ2 and CL-P1NT using a yeast two-hybrid β-galactosidase liquid culture assay. We observed the N-terminal amino acids 1-16 of CL-P1NT

were very important for the interaction between CL-P1NT and μ2 in yeast (Fig. 2B). CL-P1NT also has another putative endocytic motif, an acidic amino acid cluster at position 7-10. Mutagenesis studies of this glutamic acid cluster and tyrosine motif of CL-P1NT were carried out to identify the amino acid residues necessary for the CL-P1 and μ2 interaction in yeast. As seen in Figure 2C, the mutation of CL-P1NT residue Y16 to alanine completely inhibited the interaction of CL-P1NT with μ2 in yeast. The acidic amino acid cluster and a change of F19 to alanine slightly inhibited the interactions. These results indicate that YKRF is the important motif in supporting the interaction with μ2.

3.2. The C-terminal domain of μ2 is important for the interaction between μ2 and CL-P1

The μ2 chain has a bipartite structure: one third (residues 1-145) is the amino terminal which is seemed to be involved in the assembly of the β2 chain of the adaptor complex and two thirds (residues 164-453) at the carboxyl terminal which is involved in the binding of tyrosine-based sorting signals. The interactions between CL-P1NT and the two kinds of truncated μ2 were evaluated using a GST pull-down assay (Fig. 3A) and yeast two-hybrid β-galactosidase liquid culture assays (Fig. 3B). Fig. 3A and B demonstrated that the CL-P1NT fragment could bind to the residues 164-453 of the μ2 chain.

3.3. CL-P1-mediated ligand endocytosis occurs via a clathrin-dependent pathway

To elucidate the endocytic mechanism underlying ligand uptake by CL-P1, we first studied the uptake of mAb to the CRD of CL-P1 in CHO/CL-P1 cells. As shown in Fig. 4A, two internalization rates of fluorescent-labeled or biotin-labeled anti-CL-P1 mAb were measured. The CL-P1 protein of fluorescent-labeled carbohydrates (β-GalNAc), mAb and DiI-labeled OxLDL, bound to CL-P1-expressing cells and were endocytosed by CL-P1-expressing cells (Fig. 4B, Supplemental Movie 1 and Supplemental Fig. 1). The Supplemental Movie 1 and Fig. 4A demonstrated that DiI-labeled OxLDL was endocytosed with similar speed in the endocytosis of CL-P1 mAb. The clathrin heavy chain (CHC), which was bound to adaptin β2 molecule in clathrin-dependent endocytosis, were colocalized with anti-CL-P1 mAb in same conditioned cells (Supplemental Fig. 2). We demonstrated that OxLDLs with several oxidation incubation times (3, 6, 10, and 24h) bound to and were endocytosed in CHO/CL-P1 cells (Supplement Fig.3). Supplement Figure 3 showed that the OxLDLs with 3h-oxidation could bind CHO/CL-P1 cells at the lowest level, those with 6 and 10h-oxidation did cells at medium level, compared with the binding that with 24h-oxidation. However, we found that the uptakes of OxLDLs with 3h and 24h oxidation were almost similar. To demonstrate whether the internalization of OxLDL (red) in CHO/CL-P1 is clathrin-dependent, CL-P1-transfected cells were subjected to potassium depletion or hypertonic treatment which was known to block the assembly of coated pits and

clathrin-mediated endocytosis, respectively (16, 17). Con A staining before fixation was used as a cell surface marker during endocytosis in these experiments (Fig. 5A, Fig. 6A, Fig. 8C). OxLDL in cytoplasmic area was detected in control condition but it was not found there in K^+ depleted condition or hypertonic condition (Fig. 5). These conditions inhibited ligand endocytosis in CL-P1 transfectants and both treatments each caused an 80% reduction in the endocytosis of OxLDL (Fig. 5C). The inhibition of OxLDL endocytosis by either treatment was reversible. These data suggest that endocytosis of CL-P1 is mediated by clathrin-coated vesicles.

3.4. The tyrosine motif is required for internalization of OxLDL in CHO/CL-P1

Tyrphostin A23, a structural analog of tyrosine is an inhibitor of tyrosine kinase, and functions by binding to the active site of the enzyme. Incubation of cells in the presence of 350 μM tyrphostin A23 for 30 min led to a marked decrease in OxLDL internalization compared with that observed in control cells (Fig. 6A, B). Wortmannin, a phagocytosis inhibitor (12) or Genistein, an inhibitor of caveolae-dependent uptake (18, 19), had no effect on the endocytosis of ligands for CL-P1 (Fig. 6A, B). Supplemental Fig. 4 indicated its inhibition was dependent on the concentration of tyrphostin A23.

3.5. Functional role of Y16 in the trafficking of CL-P1

We showed in Fig. 4A that the incubation of CL-P1 transfected CHO cells with two labeled anti-CL-P1 mAb resulted in the rapid and time-dependent uptake of these Abs. Next, we demonstrated that the HeLa cells expressed with complete CL-P1, all mutated CL-P1, and the ⊿N20 deleted CL-P1 were able to bind the DiI-OxLDL (Fig. 7A). We observed the reduced uptake of DiI-OxLDL (Fig. 7B) and its surface remaining (arrows in Fig. 7B) in Y16A or ⊿N20 mutant-expressing cells, even though the same amount of DiI-OxLDL was used for testing. The confocal microscopic analysis confirmed the reduced uptake in Y16A or ⊿N20 mutant-expressing cells (Fig. 7C, D). The % cells with internalized OxLDL were significantly impaired in the N-terminal deleted CL-P1- or the Y16A and F19A mutant CL-P1-transfected cells (Fig.7E).

3.6. CL-P1-mediated endocytosis by a clathrin-, AP-2-, and dynamin-2-dependent pathway

To further characterize CL-P1-OxLDL endocytosis, we employed siRNA treatment to deplete clathrin heavy chain (CHC), each of the AP-2 subunits (α, β2 and μ2) or dynamin-2 followed by endocytosis of DiI-labeled OxLDL in CL-P1-transfected HeLa cells. Real-time RT-PCR and western blotting revealed an 80~90% depletion of CHC or the AP-2 subunits using siRNA treatment (Fig. 8A and 8B). We observed CL-P1-OxLDL uptake was significantly inhibited by all siRNA treatment and OxLDL accumulated in the plasma membrane

area in CL-P1-transfected cells (Fig. 8C). Quantification of internalized DiI-OxLDL in control cells or in CHC- or AP-2 subunits- or dynamin-2-depleted cells demonstrated that OxLDL uptake was reduced by > 60% (Fig. 8D). This suggests that CHC, AP-2 subunits and dynamin-2 are required for CL-P1-mediated OxLDL uptake.

4. Discussion

In this study, we tried to demonstrate that the clathrin-AP complex-dependent pathway regulates endocytosis of OxLDL and other ligands in CL-P1-transfected cells. There are at least three classes of sorting motifs recognized by AP complexes. First, the NPXY motif appears to be recognized by AP-2 at the plasma membrane; however, this motif also interacts with non-AP-2 clathrin adaptors to mediate internalization (20, 21). A second motif is di-leucine-based and resides in the cytoplasmic tail of proteins targeted to endosomal and lysosomal compartments (22). The third tyrosine-based motif, YXXΦ, (in which Φ is a bulky hydrophobic amino acid), found in the CL-P1 cytoplasmic domain is usually recognized by the medium subunit of AP complexes, and this motif can thus intervene in receptor cargo sorting at the plasma membrane, TGN, and in endosomes (23). We demonstrated here that the YKRF endocytosis motif in CL-P1 affects the endocytosis of OxLDL.

In an examination of the medium chain of adaptin, μ2 exhibited a specific amino acid preference (24). First, μ2 preferred arginine at the Y+2 position (YXXΦ), a feature that is found in the internalization signals of the transferrin receptor and TGN38. Mutation of the arginine residue to aspartic acid within the TGN38 signal reduced both interactions with μ2 and internalization activity. Secondly, μ2 preferred phenylalanine at the Y-2 position. Finally, it favored leucine or phenylalanine at the hydrophobic Φ position. Replacement of valine with leucine at the Φ position of the TGN38 signal, ASDYQRL, also decreased interactivity with μ2. In the case of CL-P1, we observed arginine residue at the Y+2 position and phenylalanine at hydrophobic Φ position. Figure 7 demonstrated that the replacement of phenylalanine with alanine lowered CL-P1 internalization activity. The full-length μ2 interacted with most YXXΦ signals, including those selected by μ1, μ3A, and μ3B, but the cytoplasmic tail of CL-P1 did not interact with any other medium chains in vitro (Fig. 2A).

Although the role of OxLDL in atherosclerosis development has been well characterized (25), scavenger receptor-mediated lipid particle uptake and cellular processing remain somewhat poorly understood. A recent study showed that the conventional way of oxidizing LDL (24h treatment with CuSO4) generates a ligand that is taken up by both macrophages and sinusoidal ECs of the liver, whereas mild oxidation (3h treatment with CuSO4) gave OxLDL that is similar to OxLDL found circulating in vivo, and is taken up exclusively by the liver ECs. This report suggests that the mildly modified OxLDL has a different binding and uptake pattern than the over-oxidized LDL (26, 27). We have confirmed that CL-P1 expressing CHO cells can bind and

endocytose four-pattern OxLDLs, which are modified with 3h, 6h, 10h, and 24h treatment with CuSO4 (supplemental Figure 3). Supplement Figure 3 indicates that OxLDL with 3h-oxidation (3h-OxLDL) could bind CHO/CL-P1 cells at a very low level, compared with the binding to OxLDL with 24h-oxidation (24h-OxLDL). However, we found that the uptake of OxLDL showed almost similar level between two OxLDLs with different oxidation periods. It was surprising that 3h-OxLDL were endocytosed in the similar level of 24h-OxLDL although 3h-OxLDL showed the lowest binding to CL-P1. We speculated that the LDL might become the different negatively charged and chemically modified OxLDL due to the oxidation with different time periods. On the other hand, CL-P1 as a receptor having the four functional regions of a coiled-coil domain, a collagen-like domain, a neck domain, and a carbohydrate recognition domain, in the extracellular domain, could utilize four regions as the binding domain. The utilization of the one or several binding domains might affect the endocytosis speed of the different modified OxLDLs. Furthermore, these results indicate that OxLDL with mild oxidation (3h-OxLDL) like that found circulating *in vivo*, is highly endocytosed through CL-P1 like 24h-OxLDL (26, 27). We previously demonstrated that the expression of CL-P1 mRNA was found in human liver tissues (10). These results indicate that CL-P1 might be able to be a receptor for various OxLDLs with different oxidations in human liver tissues. Further investigations are needed in order to elucidate what is dependent on a difference between the binding and uptake activity for OxLDL.

Now, it is considered that there are two pathways of endocytosis through clathrin-coated vesicle and lipid rafts/caveolae. SR-BI, was the first cell surface high density lipoprotein (HDL) receptor to be well defined at a molecular level. It mediates both the selective uptake by cells of HDL lipids (mainly cholesterol esters) as well as the cellular efflux of cholesterol into the lipoprotein pool. The immunofluorescence microscopic study revealed that SR-BI co-localized with caveolin-1 in punctate microdomains located across the cell surface and at the periphery (28). With SR-BII, however, mediation of HDL endocytosis occurs through a clathrin-dependent, caveolae-independent pathway (29). CD36 in SR-B family has been reported to be present in lipid rafts/caveolae, but its expression in caveolin-1-negative KB cell lines is sufficient for OxLDL-induced internalization of CD36, indicating that caveolin-1 is not required for this endocytic process (30). In the case of LOX-1, the endocytosis of OxLDL was mediated via a dynamin-2-dependent and clathrin-independent pathway (15). These investigations on endocytosis through the action of various scavenger receptors indicate that endocytosis was controlled by different pathways in each individual scavenger receptor and was not fixed on just one pathway.

The internalization in macrophages of AcLDL via SR-A was due to a clathrin-dependent pathway using a di-leucine motif of the SR-A intracellular domain (31). In addition, the internalization of fucoidan via SR-A required caveolae-dependent endocytosis and caused apoptosis in macrophages (32). Two reports revealed that the clathrin-dependent endocytosis of AcLDL activates ERK signaling and the caveolae-dependent pathway,

while that of fucoidan causes p38 kinase and JNK signaling as well as caspase activation. These results suggest that different endocytosis pathways via the same scavenger receptor were used and that they were dependent on the two individual ligands of AcLDL and fucoidan. To date, there has been no report to explain why macrophages used two different pathways through SR-A.

Finally, we demonstrated here an interaction between μ2 chain of AP complex and the YKRF sorting motif in the CL-P1 cytoplasmic domain and elucidated that this signal can act as an internalization signal at the plasma membrane as well as an intracellular sorting signal. In addition, its endocytosis of antibodies and sugar moieties as well as OxLDL was mediated by the clathrin-AP2 pathway and dynamin-2-dependent pathway.

Acknowledgements

*This work was supported by grants from Grants-in-Aid for Scientific Research (22390113, 26293124) and from the “Knowledge Cluster Initiative” (Sapporo Biocluster Bio-S), a project of the Japan of Ministry of Education, Culture, Sports, Science, and Technology. This work was also supported by grants from Fuso Pharmaceutical Industries, Ltd., the Smoking Research Foundation, the Takeda Science Foundation, and the Mizutani foundation for glycoscience.

References

1. Murphy, J. E., Tedbury, P. R., Homer-Vanniasinkam, S., Walker, J. H., and Ponnambalam, S. Biochemistry and cell biology of mammalian scavenger receptors. Atherosclerosis 182 (2005) 1-15.

2. Goldstein, J. L., Ho, Y. K., Basu, S. K., and Brown, M. S. Binding site on macrophages that mediates uptake and degradation of acetylated low density lipoprotein, producing massive cholesterol deposition. Proc. Natl. Acad. Sci. U. S. A. 7 (1979) 333-337.

3. Greaves, D. R., Gough, P. J., and Gordon, S. Recent progress in defining the role of scavenger receptors in lipid transport, atherosclerosis and host defence. Curr. Opin. Lipidol. 9 (1998) 425-432.

4. Acton, S. L., Scherer, P. E., Lodish, H. F., and Krieger, M. Expression cloning of SR-BI, a CD36-related class B scavenger receptor. J. Biol. Chem. 269 (1994) 21003-21009.

5. Yuhanna, I. S., Zhu, Y., Cox, B. E., Hahner, L. D., Osborne-Lawrence, S., Lu, P., Marcel, Y. L., Anderson, R. G., Mendelsohn, M. E., Hobbs, H. H., and Shaul, P. W. High-density lipoprotein binding to scavenger receptor-BI activates endothelial nitric oxide synthase. Nat. Med. 7 (2001) 853-857.

6. Li, X. A., Titlow, W. B., Jackson, B. A., Giltiay, N., Nikolova-Karakashian, M., Uittenbogaard, A., and Smart, E. J. High density lipoprotein binding to scavenger receptor, Class B, type I activates endothelial nitric-oxide synthase in a ceramide-dependent manner. J. Biol. Chem. 277 (2002) 11058-11063.

7. Sawamura, T., Kume, N., Aoyama, T., Moriwaki, H., Hoshikawa, H., Aiba, Y., Tanaka, T., Miwa, S., Katsura, Y., Kita, T., and Masaki, T. An endothelial receptor for oxidized low-density lipoprotein. Nature 386 (1997) 73-77.

8. Adachi, H., Tsujimoto, M., Arai, H., and Inoue, K. Expression cloning of a novel scavenger receptor from human endothelial cells. J. Biol. Chem. 272 (1997) 31217-31220.

9. Sørensen, K. K., McCourt, P., Berg, T., Crossley, C., Le Couteur, D., Wake, K., Smedsrød, B. The scavenger endothelial cell: a new player in homeostasis and immunity. Am J Physiol Regul Integr Comp Physiol. 303(2012) R1217-1230.

10. Ohtani, K., Suzuki Y., Eda S., Kawai T., Kase T., Keshi H., Sakai Y., Fukuoh A., Sakamoto T., Itabe H., Suzutani T., Ogasawara M., Yoshida I., and Wakamiya N. The membrane-type collectin CL-P1 is a scavenger receptor on vascular endothelial cells. J. Biol. Chem. 276 (2001) 44222-44228.

11. Kodama, T., Freeman, M., Rohrer, L., Zabrecky, J., Matsudaira, P., and Krieger, M. Type I macrophage scavenger receptor contains alpha-helical and collagen-like coiled coils. Nature 343 (1990) 531-535.

12. Jang S., Ohtani K., Fukuoh A., Yoshizaki T., Fukuda M., Motomura W., Mori K., Fukuzawa J., Kitamoto N., Yoshida I., Suzuki Y., and Wakamiya N. Scavenger receptor collectin placenta 1 (CL-P1) predominantly mediates zymosan phagocytosis by human vascular endothelial cells. J. Biol. Chem. 284 (2009) 3956-3965.

13. Koyama, S., Ohtani, K., Fukuzawa, J., Yao N., Fukuda, M., Jang, S., Hasebe, N., Kikuchi, K., Itabe, H.,

Yoshida, I., Suzuki, Y., and Wakamiya, N. The induction of human CL-P1 expression in hypoxia/reoxygenation culture condition and rat CL-P1 after ischemic/reperfusion treatment. Biochim. Biophys. Acta. 1810 (2011) 836-842.

14. Traub, L. M. Tickets to ride: selecting cargo for clathrin-regulated internalization. Nat. Rev. Mol. Cell Biol. 10 (2009) 583-596.

15. Murphy, J. E., Vohra, R. S., Dunn, S., Holloway, Z. G., Monaco, A. P., Homer-Vanniasinkam, S., Walker J. H., and Ponnambalam, S. Oxidised LDL internalisation by the LOX-1 scavenger receptor is dependent on a novel cytoplasmic motif and is regulated by dynamin-2. J. Cell Sci. 121 (2008) 2136-2147.

16. Larkin, J. M., Brown, M. S., Goldstein, J. L., and Anderson, R. G. Depletion of intracellular potassium arrests coated pit formation and receptor-mediated endocytosis in fibroblasts. Cell 33 (1983) 273-285.

17. Hansen, S. H., Sandvig, K. and van Deurs, B. Clathrin and HA2 adaptors: effects of potassium depletion, hypertonic medium, and cytosol acidification. J. Cell Biol. 121 (1993) 61-72.

18. Tiruppathi, C., Song, W., Bergenfeldt, M., Sass, P. and Malik, A. B. Gp60 activation mediates albumin transcytosis in endothelial cells by tyrosine kinase-dependent pathway. J. Biol. Chem. 272 (1997) 25968-25975.

19. Pelkmans, L., Puntener, D. and Helenius, A. Local actin polymerization and dynamin recruitment in SV40-induced internalization of caveolae. Science 296 (2002) 535-539.

20. Chen W. J., Goldstein, J. L., and Brown, M. S. NPXY, a sequence often found in cytoplasmic tails, is required for coated pit-mediated internalization of the low density lipoprotein receptor. J. Biol. Chem. 265 (1990) 3116-3123.

21. Harasaki, K., Lubben, N. B., Harbour, M., Taylor, M. J., and Robinson, M. S. Sorting of major cargo glycoproteins into clathrin-coated vesicles. Traffic 6 (2005) 1014-1026.

22. Bonifacino, J. S. and Traub, L. M. Signals for sorting of transmembrane proteins to endosomes and lysosomes. Annu. Rev. Biochem. 72 (2003) 395-447.

23. Rapoport, I., Miyazaki, M., Boll, W., Duckworth, B., Cantley, L. C., Shoelson, S., and Kirchhausen, T. Regulatory interactions in the recognition of endocytic sorting signals by AP-2 complexes. EMBO J. 16 (1997) 2240-2250.

24. Ohno, H., Aguilar, R. C., Yeh, D., Taura D., Saito, T., and Bonifacino, J. S. The medium subunits of adaptor complexes recognize distinct but overlapping sets of tyrosine-based sorting signals. J. Biol. Chem. 273 (1998) 25915-25921.

25. Steinberg, D. Low density lipoprotein oxidation and its pathobiological significance. J Biol. Chem. 272(1997) 20963-20966.

26. Li, R., Oteiza, A., Sørensen, K. K., McCourt, P., Olsen, R., Smedsrød, B., Svistounov, D. Role of liver sinusoidal endothelial cells and stabilins in elimination of oxidized low-density lipoproteins. Am. J. Physiol.

Gastrointest. Liver Physiol. 300(2011) G71-81.

27. Oteiza, A., Li, R., McCuskey, R. S., Smedsrød, B., Sørensen, K. K. Effects of oxidized low-density lipoproteins on the hepatic microvasculature. Am. J. Physiol. Gastrointest. Liver Physiol. 301(2011) G684-93.

28. Babitt, J., Trigatti, B., Rigotti, A., Smart, E. J., Anderson, R. G. W., Xu S., and Krieger M. Murine SR-BI, a high density lipoprotein receptor that mediates selective lipid uptake, is N-glycosylated and fatty acylated and colocalizes with plasma membrane caveolae. J. Biol. Chem. 272 (1997) 13242-13249.

29. Eckhardt, E. R., Cai, L., Shetty, S., Zhao, Z., Szanto, A., Webb, N. R., and Van der Westhuyzen, D. R. High density lipoprotein endocytosis by scavenger receptor SR-BII is clathrin-dependent and requires a carboxyl-terminal dileucine motif. J. Biol. Chem. 281 (2006) 4348-4353.

30. Zeng, Y., Tao, N., Chung, K. N., Chung, K.-N., Heuser, J. E., and Lublin, D. M. Endocytosis of oxidized low density lipoprotein through scavenger receptor CD36 utilizes a lipid raft pathway that does not require caveolin-1. J. Biol. Chem. 278 (2003) 45931-45936.

31. Chen, Y., Wang, X., Ben, J., Yue, S., Bai, H., Guan, X., Bai, X., Jiang, L., Ji, Y., Fan, L., and Chen, Q. The di-leucine motif contributes to class a scavenger receptor-mediated internalization of acetylated lipoproteins. Arter. Thromb. Vasc. Biol. 26 (2006) 1317-1322.

32. Zhu, X., Zhuang, Y., Ben, J., Qian, L., Huang, H., Bai, H., Sha, J., He, Z., Chen, Q. Caveolae-dependent endocytosis is required for class A macrophage scavenger receptor-mediated apoptosis in macrophages. J. Biol. Chem. 286 (2011) 8231-8239.

FIGURE LEGENDS

Fig 1. Yeast two-hybrid screening of the cytoplasmic domain of CL-P1. *A,* Multiple sequence alignment of known amino acids of CL-P1 and transferrin receptor (TfR) cytoplasmic domains (h, human; m, mouse; z, zebrafish). The YKRF endocytosis motif in red frame is completely conserved in endocytosis motif among different animal CL-P1s. *B,* Yeast two hybrid analysis revealed that AP-2 μ2 interacts with the cytoplasmic domain of CL-P1 (CL-P1NT). The blue colonies containing the β-galactosidase reporter activities (X-alpha-gal), demonstrated the positive interaction in its assay. p53 (murine) and T-antigen (SV40 large T-antigen) used as a positive control but lamin C (human) as a negative one.

Fig. 2. Interaction of CL-P1NT with the medium chain of adaptor protein 2 (AP-2 μ2). *A,* The pull down assay revealed the binding of medium chains of adaptin complexes to CL-P1NT. Medium chains of several adaptins were translated in the presence of ^{35}S-methionine using the TNT system. *In vitro* translated medium chains of adaptins were incubated with glutathione-agarose beads containing GST-CL-P1NT or GST alone. The agarose precipitates or aliquots of lysates were analyzed by SDS-PAGE. *B,* Interaction of several truncated CL-P1NTs with μ2 in a yeast two-hybrid system. Interaction activity was assessed by above β-galactosidase assay and a liquid β-galactosidase assay. DDXXEEEE, acidic amino acid cluster; S, Ser/Thr protein kinase motif; YKRF, tyrosine-based motif. *C,* Interaction of various mutants of human CL-P1NT with human μ2. Wild type μ2 fused to the Gal4 activation domain was co-expressed in the yeast AH109 strain with various mutants of the cytoplasmic tail of human CL-P1 fused to the complementary Gal4 DNA binding domain. The interaction was assessed similar two β-galactosidase assay.

Fig. 3. Interaction of CL-P1NT with truncated types of μ2. *A,* The pull down assay revealed the binding of CL-P1NT to truncated types of μ2 chain. Above *In vitro* translated several kinds of truncated μ2 proteins were incubated with GST-CL-P1NT or GST alone. The precipitates and lysate aliquots were analyzed by SDS-PAGE. Luciferase was used as a negative control in the protein interaction. *B,* Interaction of CL-P1NT with truncated μ2 proteins in a yeast two-hybrid system. The cytoplasmic tail of human CL-P1 (CL-P1NT) fused to the Gal4 DNA binding domain was co-expressed with various mutants of AP-2 μ2 fused to the complementary Gal4 activation domain in the yeast. The interaction was assessed two β-galactosidase assay. Lamin C was used as a negative control.

Fig. 4. CL-P1-mediated ligand endocytosis. *A,* Kinetics of CL-P1 internalization using an anti-CL-P1 mAb (biotin-labeled or Alexa Fluor 488-conjugated) with CHO/CL-P1 cells. The symbol of closed triangle indicates

internalized biotin-mAb and that of closed square indicates internalized fluorescence values. *B*, OxLDL colocalization with CL-P1. CL-P1-expressing CHO cells were incubated with fluorescent-labeled ligands (Green, Alexa Fluor 488-conjugated anti-CL-P1 mAb; Red, DiI-labeled OxLDL) on ice for 1 h and then warmed to 37°C for the indicated times (0, 10, 30, 60, 90 min) before fixation. Asterisks indicate cell nuclei. Scale bar: 20 μm.

Fig. 5. CL-P1-mediated DiI-OxLDL endocytosis occurs via a clathrin-dependent pathway. *A*, CL-P1-expressing CHO cells were incubated with DiI-OxLDL (red) in control or potassium-free buffer. The plasma membrane was labeled with FITC-Con A as cell surface marker (green) and nuclei were stained with Hoechst 33342 (blue) immediately before fixation. Scale bar: 20 μm. *B*, Potassium-depletion or hypertonic treatment was reversible. Addition of exogeneous 10 mM KCl or normal media (recovery) for 1 h restored the inhibitory effect on DiI-OxLDL uptake. Asterisks indicate cell nuclei. *C*, The percentage of cells internalized DiI-OxLDL after above treatments was determined. Data represent means±s.e.m. (n=3 experiments). The *P* values were calculated relative to control values (untreated), $^{**}P<0.001$.

Fig. 6. Uptake of DiI-OxLDL by CL-P1-expressing cells with several inhibitors. Inhibitors were first treated with 200 nM wortmannin, 100 μM genistein, 350 μM tyrphostin A23. *A*, CL-P1-expressing CHO cells were incubated with DiI-OxLDL (red). There is FITC-Con A (green) as surface marker and Hoechst 33342 (blue) as nuclear marker. The endocytosis was inhibited by only tyrphostin A23. Scale bar: 20 μm. *B*, The percentage of transfected cells with internalized DiI-OxLDL was determined. Data represent means±s.e.m. (n=3 experiments). The *P* values were calculated relative to the control values (untreated), $^{**}P<0.001$.

Fig. 7. Uptake of OxLDL by CL-P1 N-terminal mutant-expressing HeLa cells. The OxLDL binding and uptake were monitored by fluorescence microscopy. *A*, Binding of DiI-OxLDL (red) in CL-P1-transfected HeLa cells with amino acid substitutions (E7,8A, E9,10A, S13A, Y16A, F19A) and its deletion (⊿N20), *B*, Endocytosis of DiI-OxLDL (red) in CL-P1-transfected HeLa cells with same amino acid substitutions and its deletion. Arrows indicate internalized DiI-OxLDL and the arrowhead indicates plasma membrane DiI-OxLDL accumulation in cells. Scale bar: 50 μm. *C*, The binding of OxLDL and anti-CL-P1 mAb (Red, DiI-OxLDL; Green, Alexa Fluor 488-conjugated anti-CL-P1 mAb) was monitored by confocal laser microscopy. Z-axis image view of ligand-binding in CL-P1-transfected HeLa cells without amino acid substitutions. *D*, The uptake of labeled ligands (Red, DiI-OxLDL; Green, Alexa Fluor 488-conjugated anti-CL-P1 mAb) was similarly monitored. Z-axis image view of ligand-internalization in same cells without or with amino acid substitutions (Y16A) and its deletion (⊿N20). Nuclei were stained with Hoechst 33342 (blue). Scale bar: 20 μm. *E*, The percentage of transfected cells with internalized DiI-OxLDL was determined. Data represent means±s.e.m.

(n=3 separate experiments, 50 cells from each experiment). *P* values were calculated relative to the control, **P*<0.05; ***P*<0.01.

Fig. 8. Clathrin-, AP-2- and dynamin-2-dependent uptake of OxLDL by CL-P1. *A and B,* HeLa cell subjected to RNAi through a scrambled siRNA negative control (mock), a siRNA duplex specific for the clathrin heavy chain (CHC), siRNAs for AP-2 adaptor complex, or dynamin-2 on cells expressing CL-P1. Real time-PCR and western blotting to demonstrate the depletion of endogenous mRNA and protein levels after RNAi treatment using the mock control (MOCK or CL-P1), CHC siRNA (CHC), α siRNA (AP2A1), β2 siRNA (AP2B1), μ2 siRNA (AP2M1), dynamin-2 SiRNA (DYN2), and positive control (Actin). *C,* Following RNAi, the uptake of labeled ligands was monitored by fluorescence microscopy. There is FITC-Con A (green) as surface marker and Hoechst 33342 (blue) as nuclear marker. Arrows indicate internalized DiI-OxLDL (red) in MOCK and the arrowhead indicates plasma membrane DiI-OxLDL accumulation in cells after above all RNAi treatments. Scale bar: 20 μm. *D,* Quantification of uptake of DiI-OxLDL in them (n=3 separate experiments, 50 cells from each experiment, error bar indicates s.e.m.) was carried out as described in Materials and Methods. The *P* values were calculated relative to control values (untreated), ***P*<0.01.

Figure

A

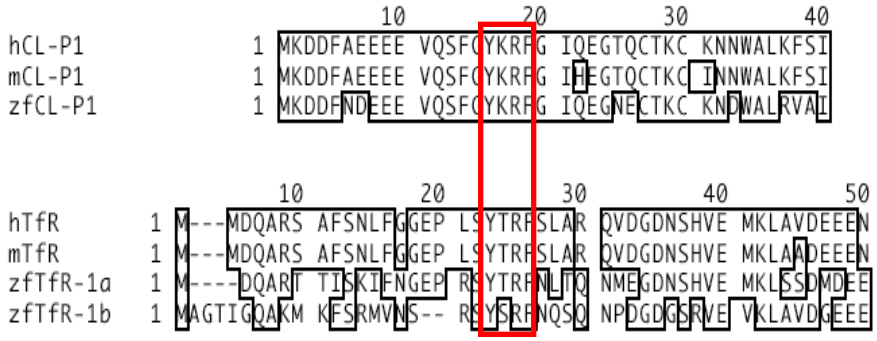

B

Bait	Pray	X-α-gal
p-53	T-antigen	
Lamin C	μ2	
CL-P1NT	μ2	

Figure 1.

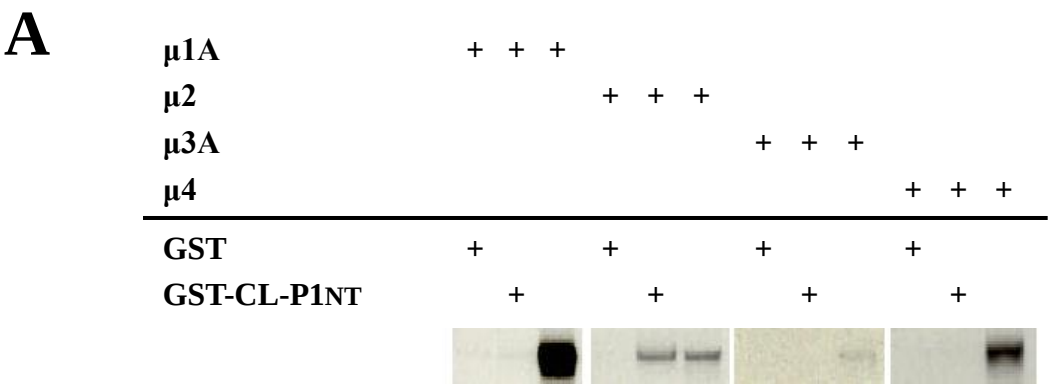
A
μ1A + + +
μ2 + + +
μ3A + + +
μ4 + + +
GST + + + +
GST-CL-P1NT + + + +

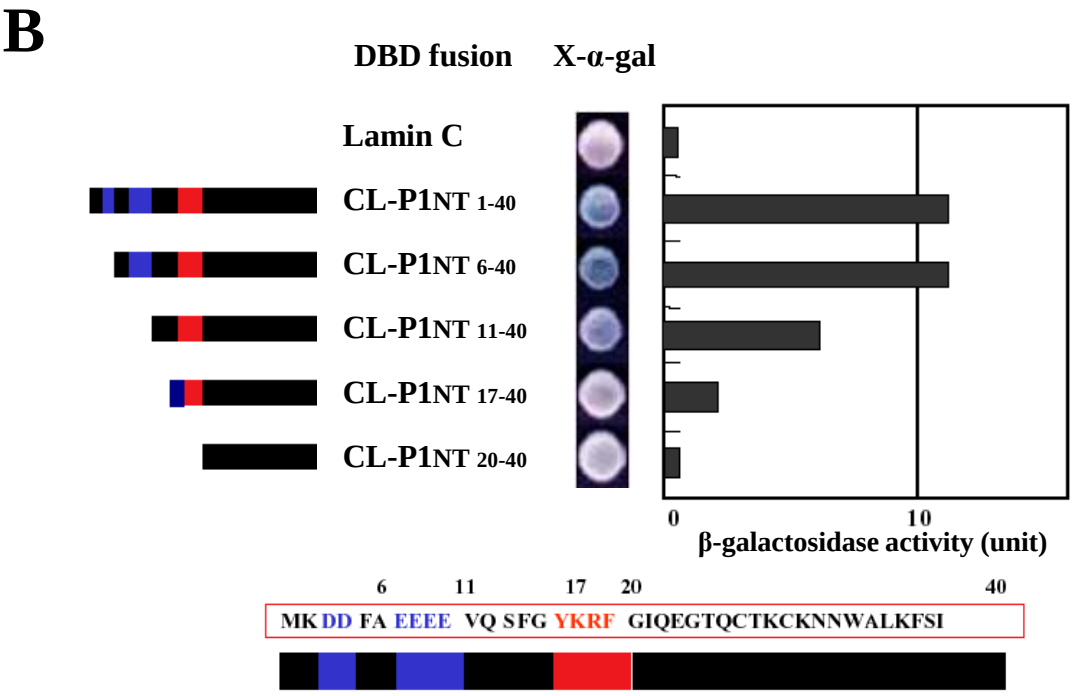
B
DBD fusion
X-α-gal
Lamin C
CL-P1NT 1-40
CL-P1NT 6-40
CL-P1NT 11-40
CL-P1NT 17-40
CL-P1NT 20-40
0
10
β-galactosidase activity (unit)
6
11
17
20
40
MK DD FA EEEE VQ SFG YKRF GIQEGTQCTKCKNNWALKFSI

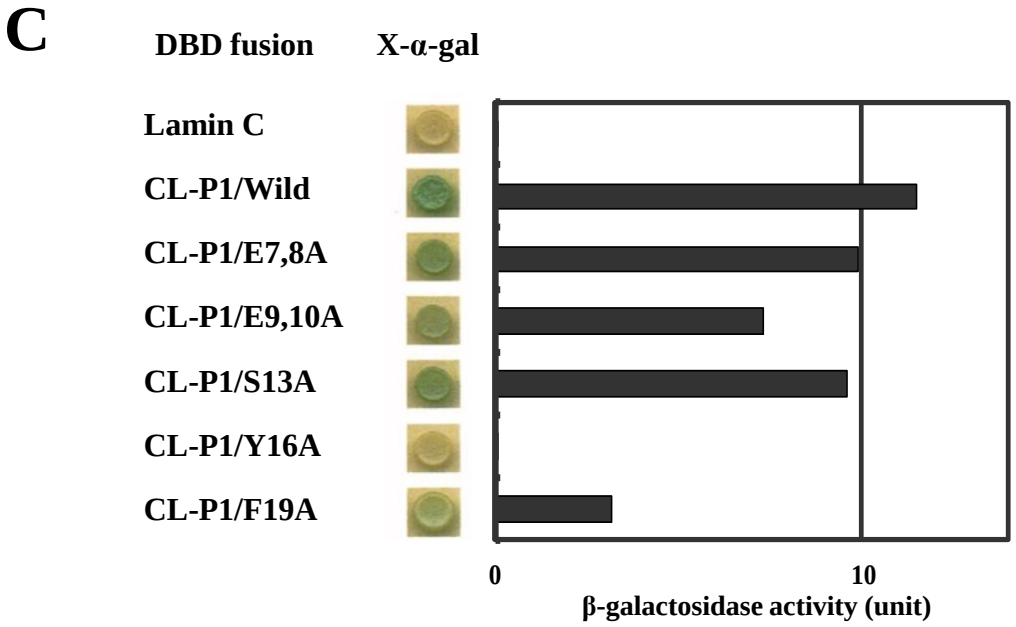
C
DBD fusion
X-α-gal
Lamin C
CL-P1/Wild
CL-P1/E7,8A
CL-P1/E9,10A
CL-P1/S13A
CL-P1/Y16A
CL-P1/F19A
0
10
β-galactosidase activity (unit)

Figure 2.

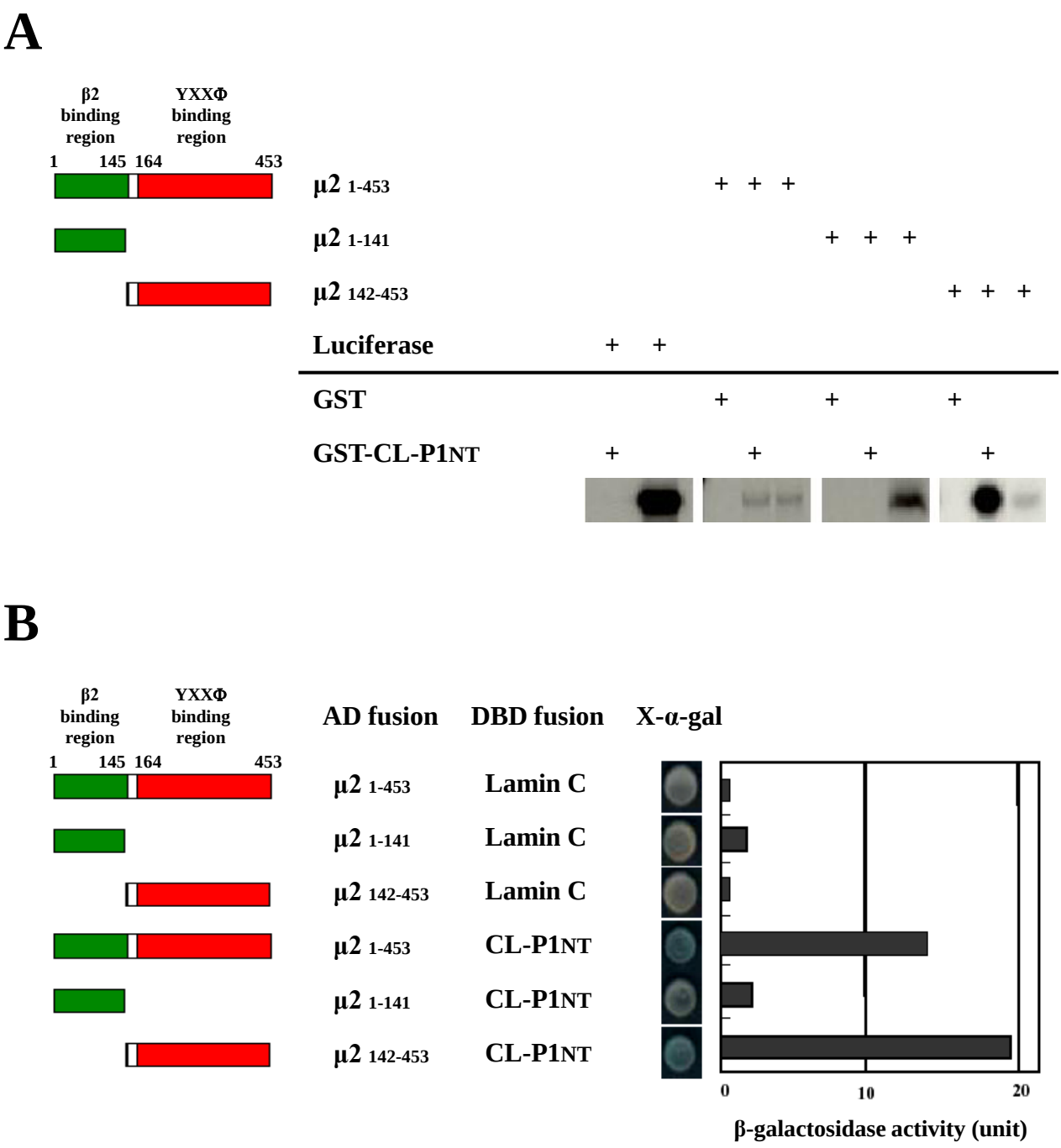
A
β2 binding region
YXXΦ binding region
1
145
164
453
μ2 1-453
μ2 1-141
μ2 142-453
Luciferase
GST
GST-CL-P1NT
B
β2 binding region
YXXΦ binding region
1
145
164
453
AD fusion
DBD fusion
X-α-gal
μ2 1-453
Lamin C
μ2 1-141
Lamin C
μ2 142-453
Lamin C
μ2 1-453
CL-P1NT
μ2 1-141
CL-P1NT
μ2 142-453
CL-P1NT
0
10
20
β-galactosidase activity (unit)

Figure 3.

A

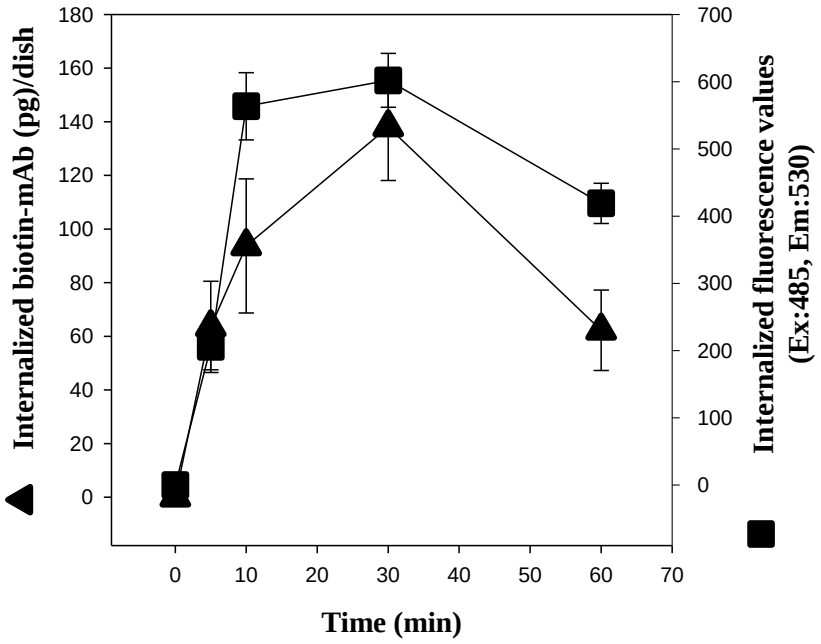
Internalized biotin-mAb (pg)/dish
180
160
140
120
100
80
60
40
20
0
700
600
500
400
300
200
100
0
Internalized fluorescence values
(Ex:485, Em:530)
0
10
20
30
40
50
60
70
Time (min)

Figure 4.

B

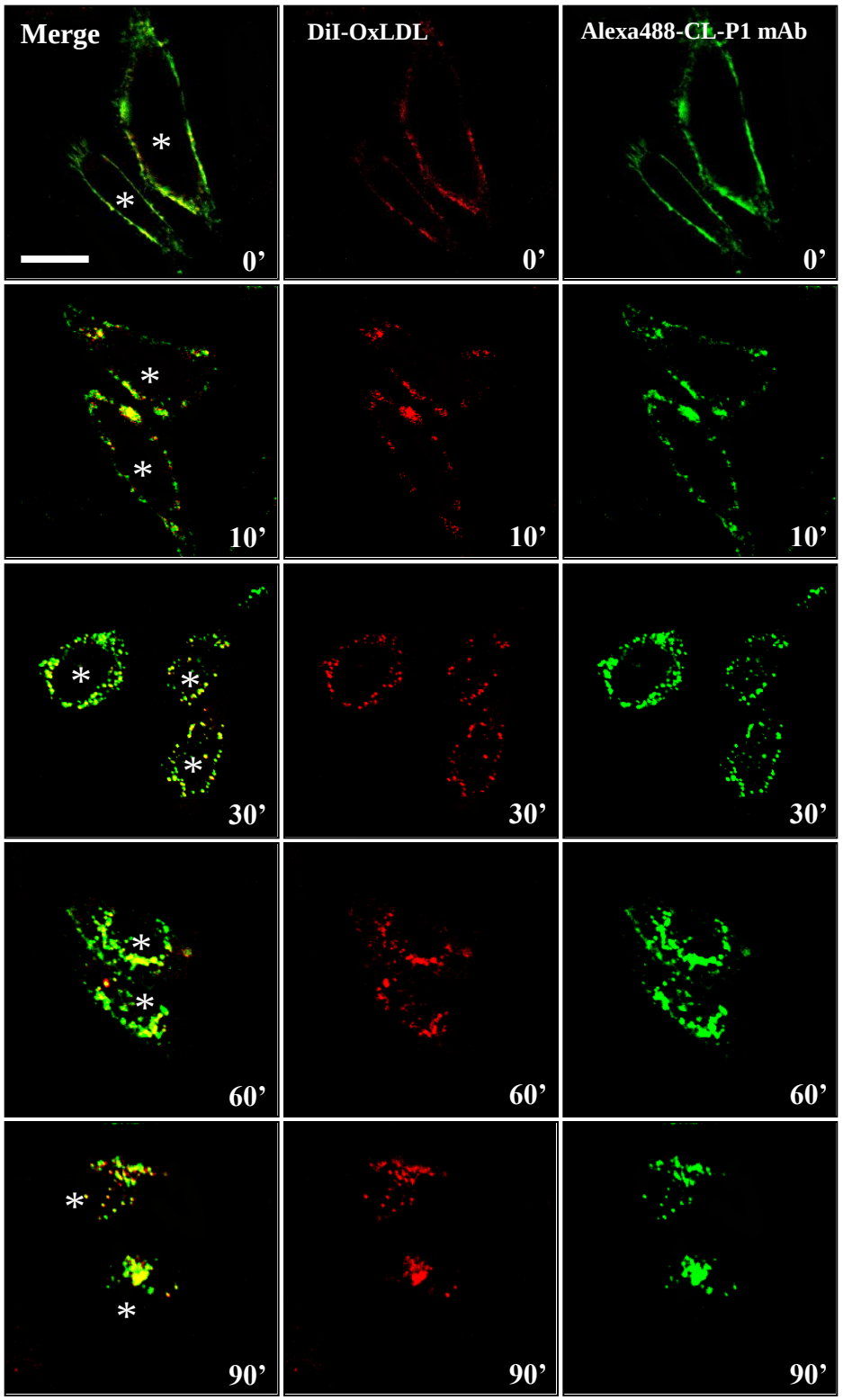

Figure 4.

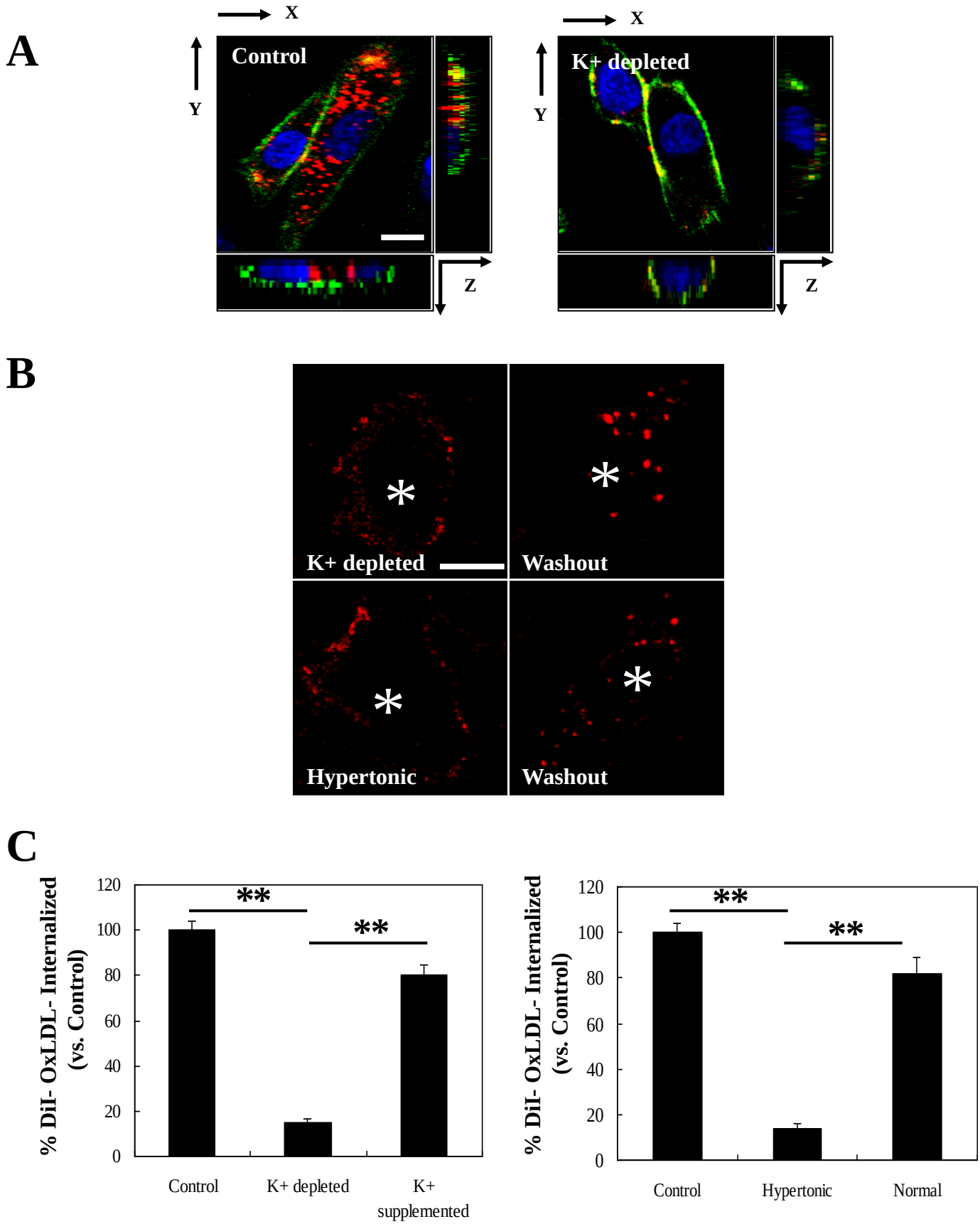
A
X
Y
Control
Z
X
Y
K+ depleted
Z
B
K+ depleted
Washout
Hypertonic
Washout
C
% DiI- OxLDL- Internalized (vs. Control)
120
100
80
60
40
20
0
**
**
Control
K+ depleted
K+ supplemented
% DiI- OxLDL- Internalized (vs. Control)
120
100
80
60
40
20
0
**
**
Control
Hypertonic
Normal

Figure 5.

A

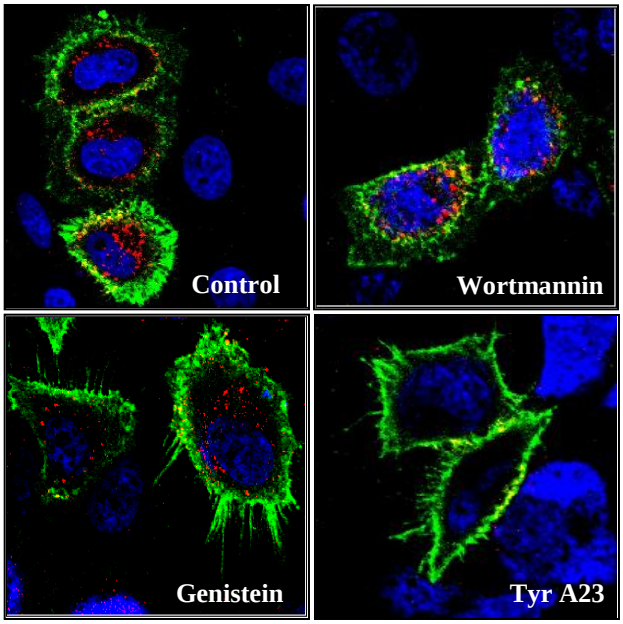
Control
Wortmannin
Genistein
Tyr A23

B

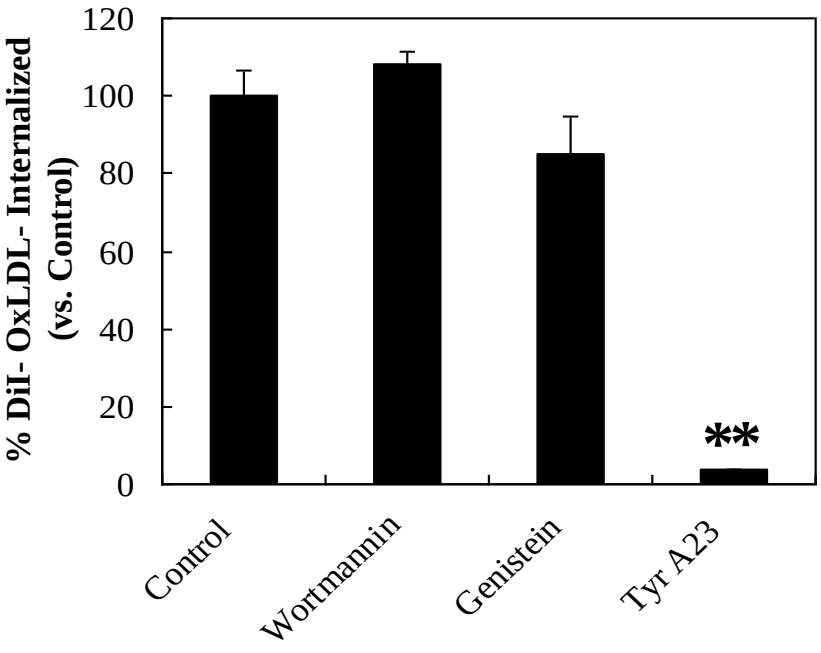
% DiI- OxLDL- Internalized
(vs. Control)
120
100
80
60
40
20
0
**
Control
Wortmannin
Genistein
Tyr A23

Figure 6.

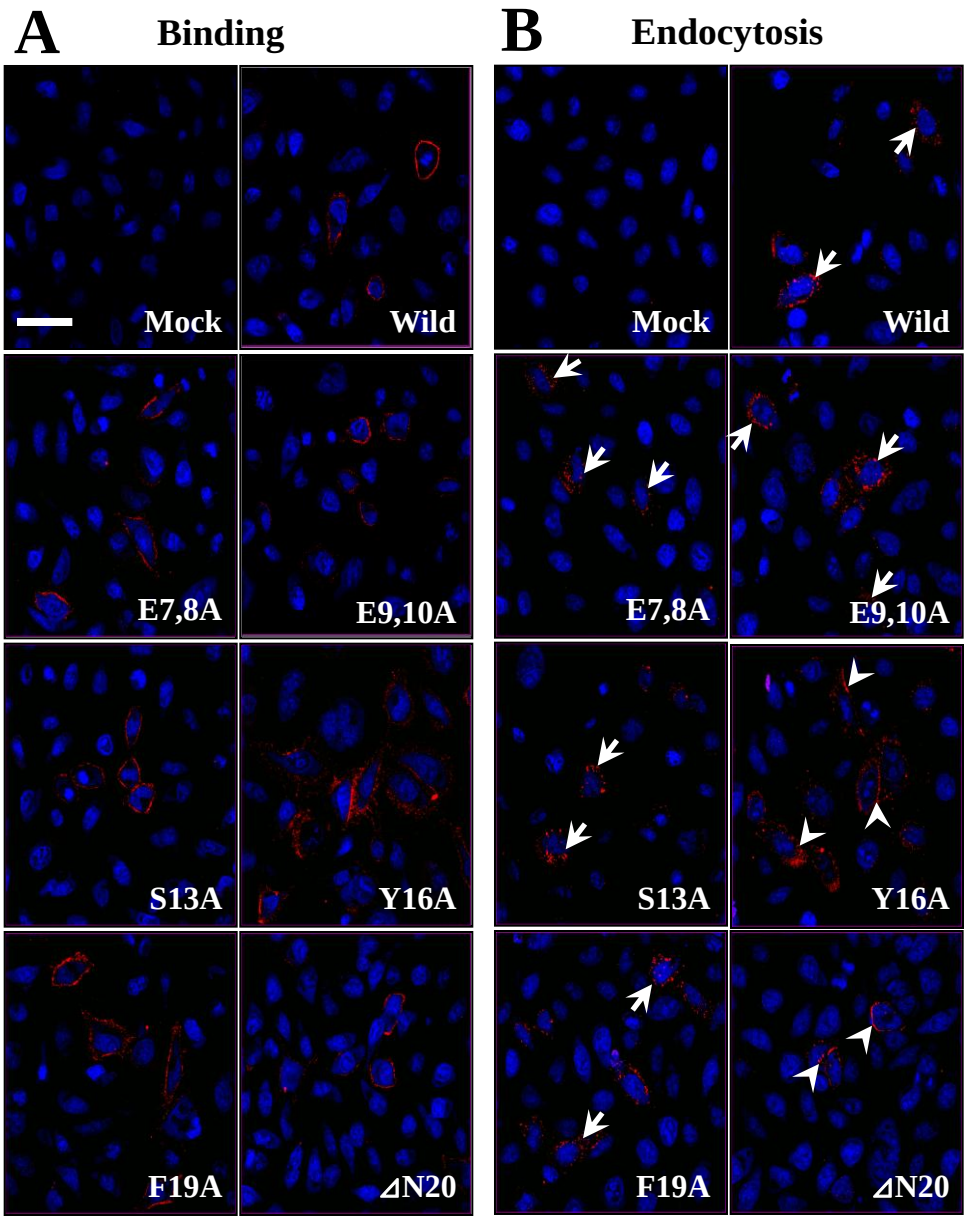
A
Binding
B
Endocytosis
Mock
Wild
Mock
Wild
E7,8A
E9,10A
E7,8A
E9,10A
S13A
Y16A
S13A
Y16A
F19A
⊿N20
F19A
⊿N20

Figure 7.

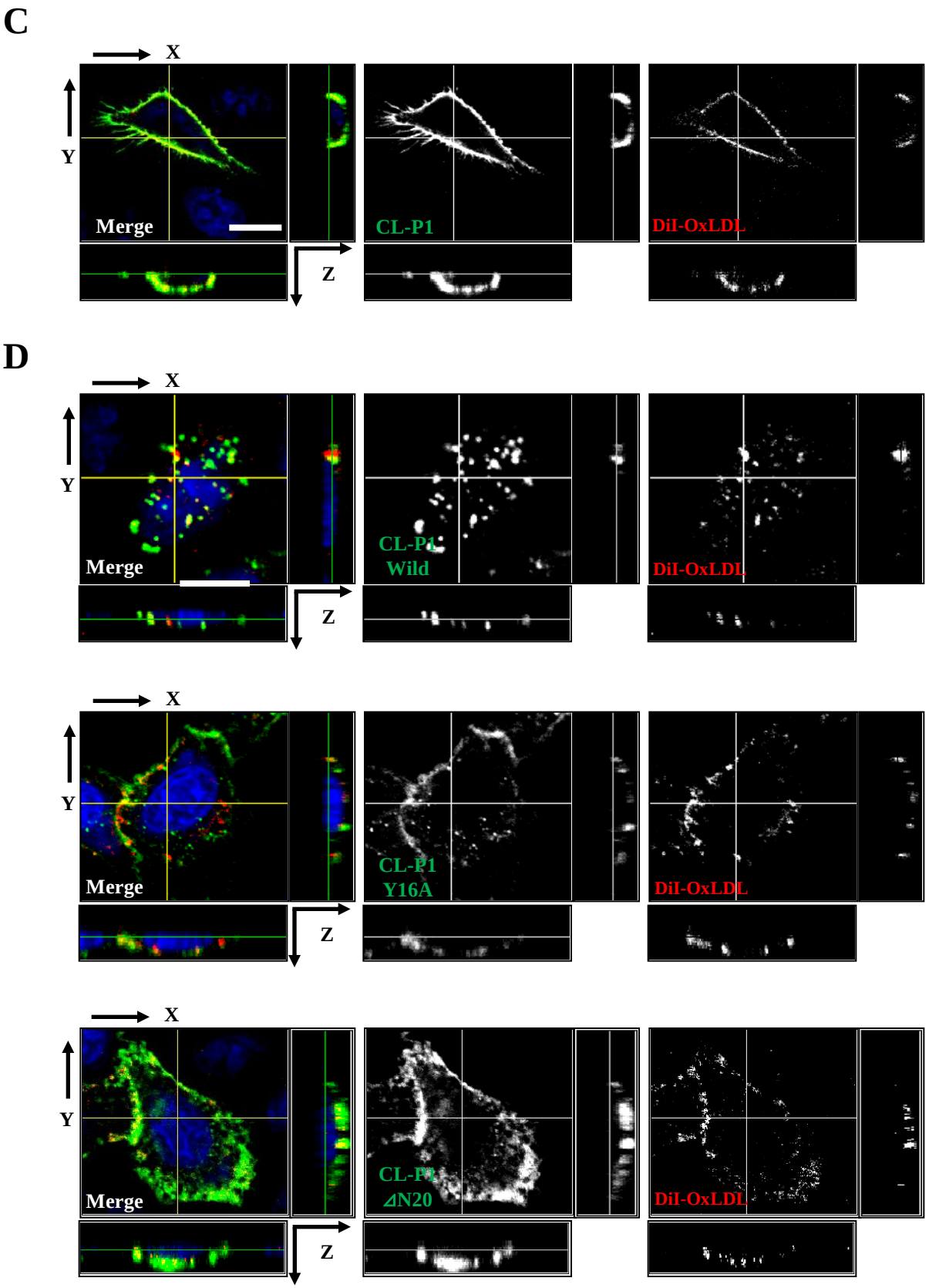
C
X
Y
Merge
CL-P1
DiI-OxLDL
Z
D
X
Y
Merge
CL-P1
Wild
DiI-OxLDL
Z
X
Y
Merge
CL-P1
Y16A
DiI-OxLDL
Z
X
Y
Merge
CL-P1
⊿N20
DiI-OxLDL
Z

Figure 7.

E

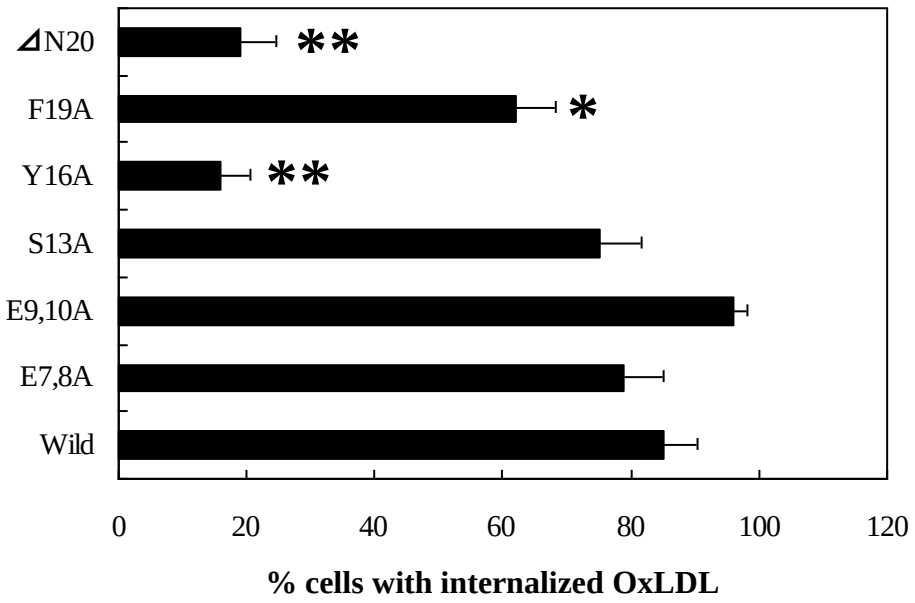
⊿N20
F19A
Y16A
S13A
E9,10A
E7,8A
Wild
**
*
**
0
20
40
60
80
100
120
% cells with internalized OxLDL

Figure 7.

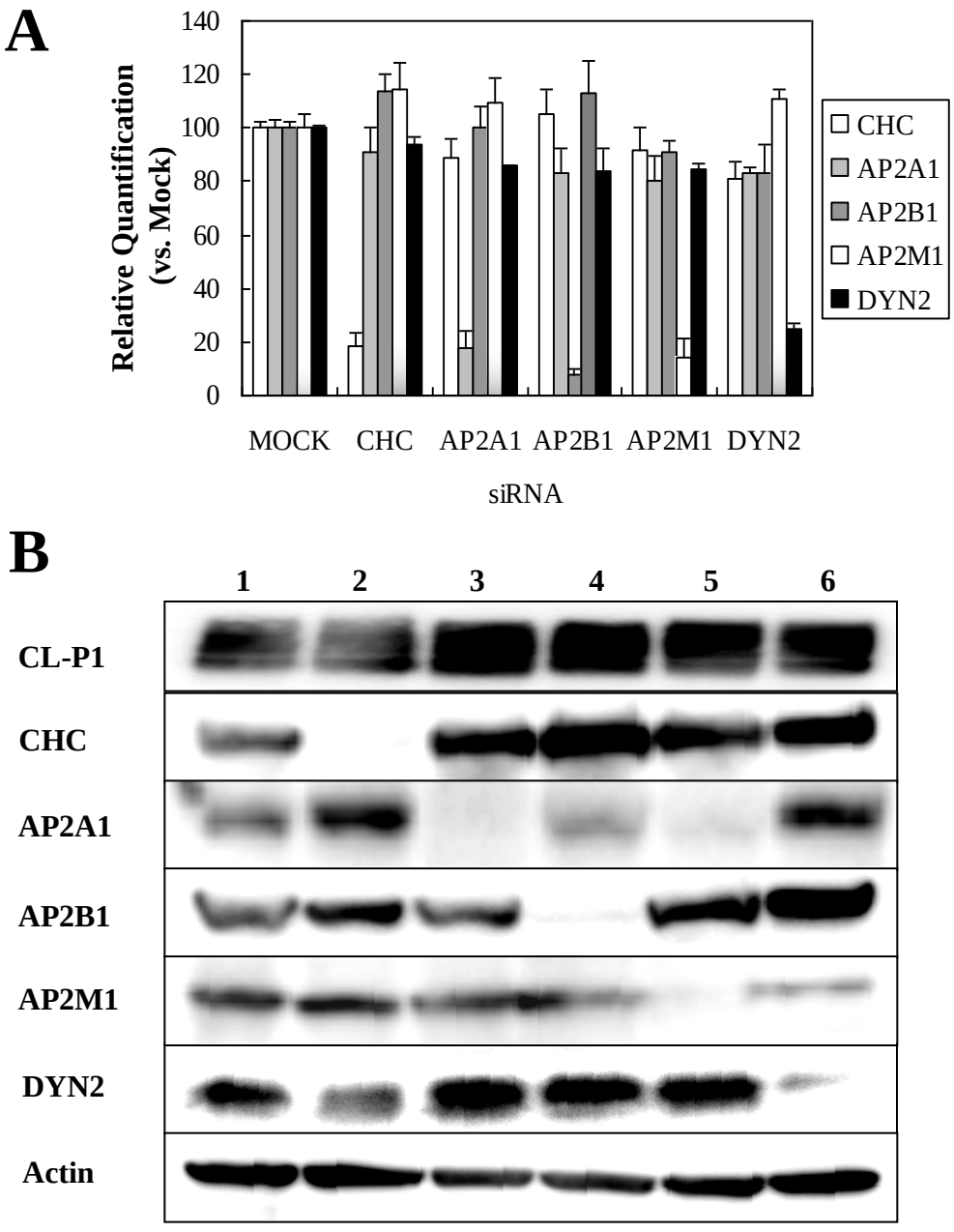
A
Relative Quantification (vs. Mock)
140
120
100
80
60
40
20
0
CHC
AP2A1
AP2B1
AP2M1
DYN2
MOCK
CHC
AP2A1
AP2B1
AP2M1
DYN2
siRNA
B
1
2
3
4
5
6
CL-P1
CHC
AP2A1
AP2B1
AP2M1
DYN2
Actin

Figure 8.

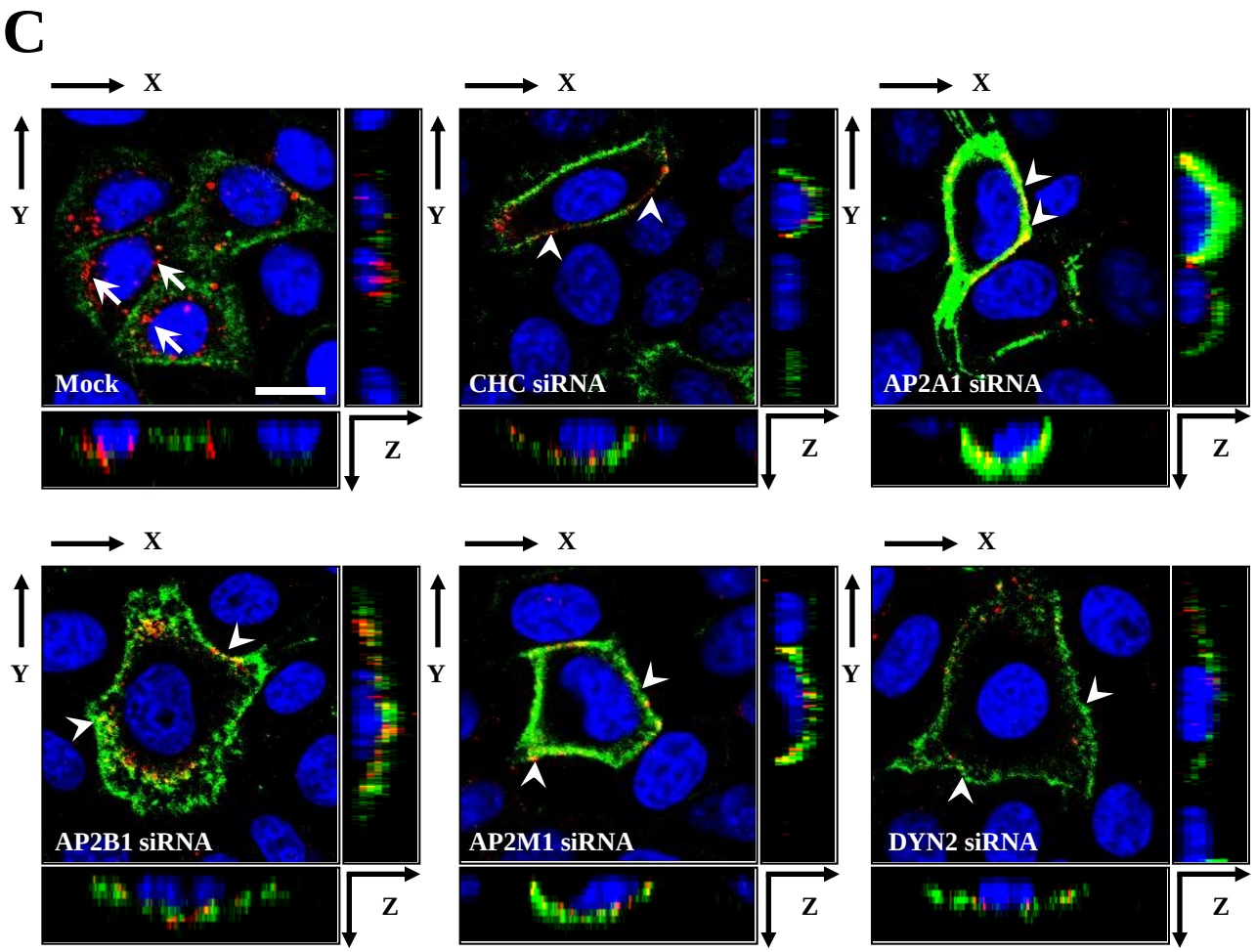
C
X
Y
Z
Mock
CHC siRNA
AP2A1 siRNA
AP2B1 siRNA
AP2M1 siRNA
DYN2 siRNA

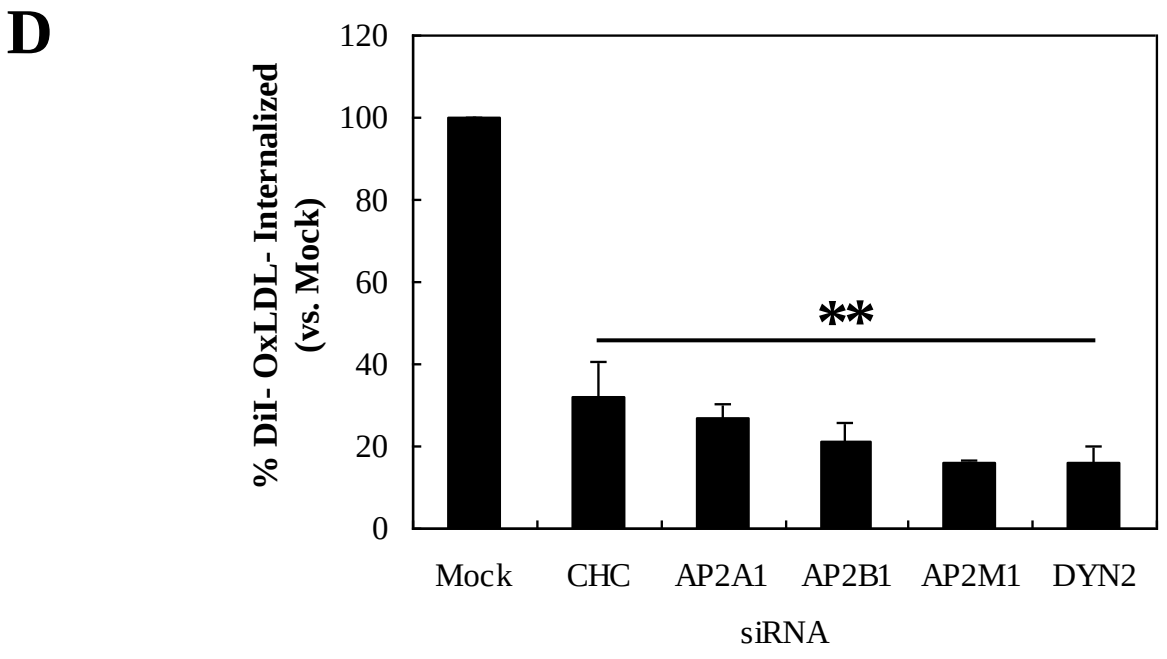
D
% DiI- OxLDL- Internalized
(vs. Mock)
120
100
80
60
40
20
0
**
Mock
CHC
AP2A1
AP2B1
AP2M1
DYN2
siRNA

Figure 8.

Supplemental Figure 1

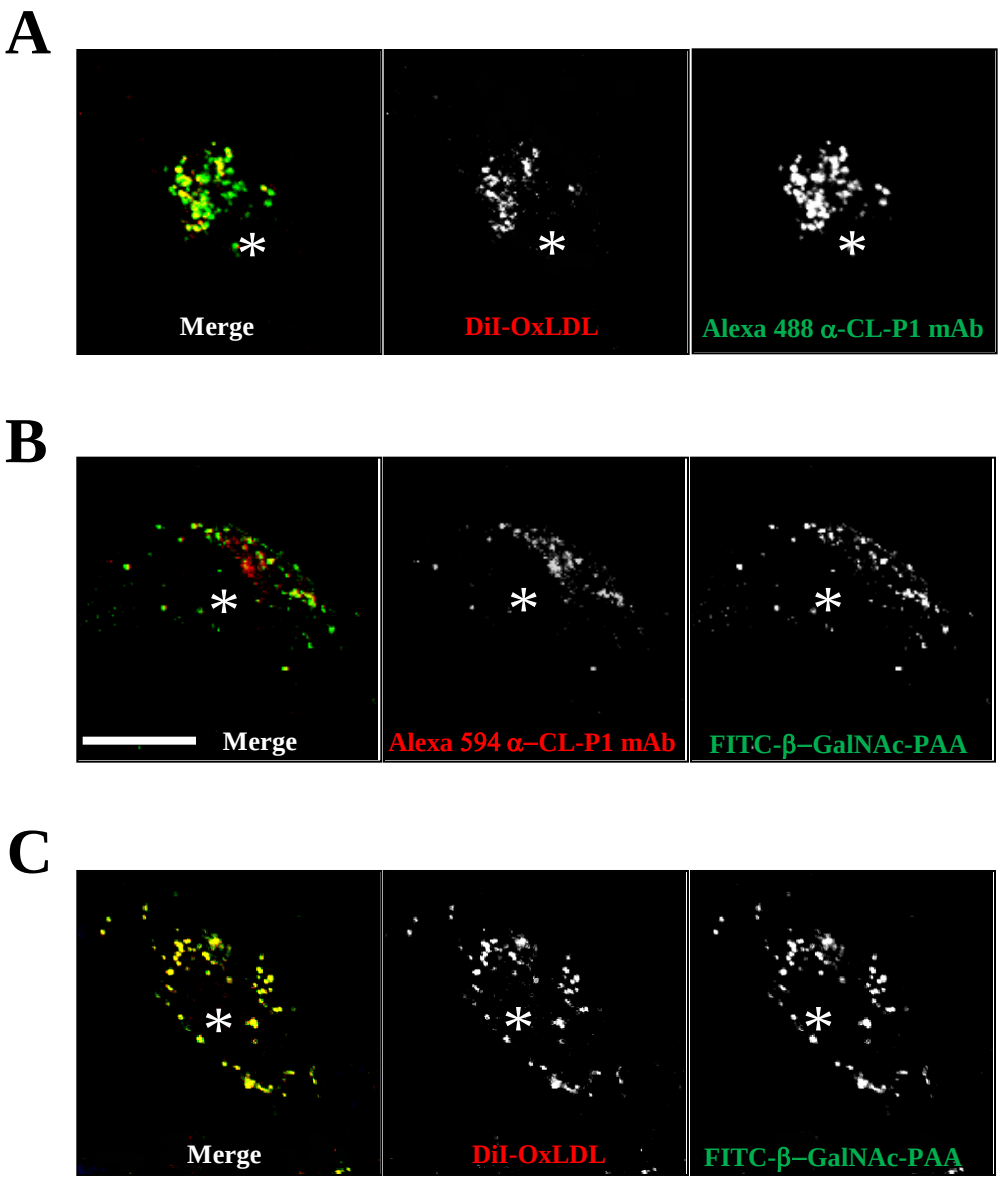

S1. Internalization of several CL-P1 ligands in CHO/CL-P1 cells. (A) DiI-labeled OxLDL with anti-CL-P1 mAb, (B) FITC-β-GalNAc-PAA with Alexa Fluor 594-conjugated anti-CL-P1 mAb, (C) DiI-labeled OxLDL with FITC-β-GalNac-PAA. CHO/CL-P1 cells were pre-incubated with anti-CL-P1 mAb on ice, then warmed to 37°C 1 h before fixation. Asterisks indicate cell nuclei. Scale bar: 20 μm.

Supplemental Figure 2

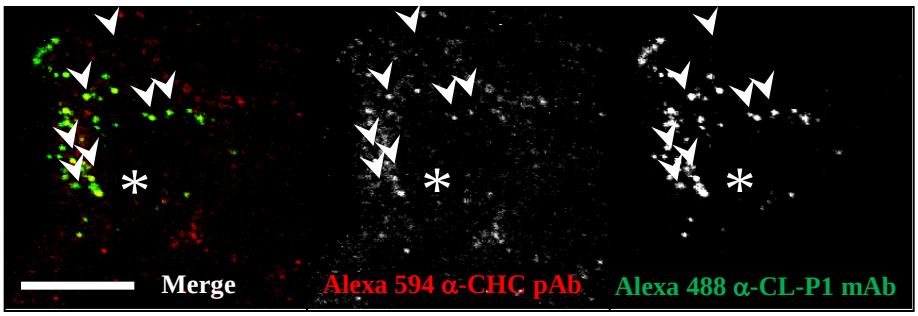

S2. CL-P1 colocalized with clathrin. CHO/CL-P1 cells were pre-incubated with anti-CL-P1 mAb on ice, then warmed to 37°C followed by fixation, permeabilization and labeling with rabbit anti-clathrin antibodies followed by treatment with Alexa Fluor 488-conjugated anti-mouse IgG antibodies (green) and Alexa Fluor 594-conjugated anti-rabbit IgG antibodies (red). Arrowheads indicate endocytic coated pits in cells. Asterisks indicate cell nuclei. Scale bar: 20 μm.

Supplement Fig. 3

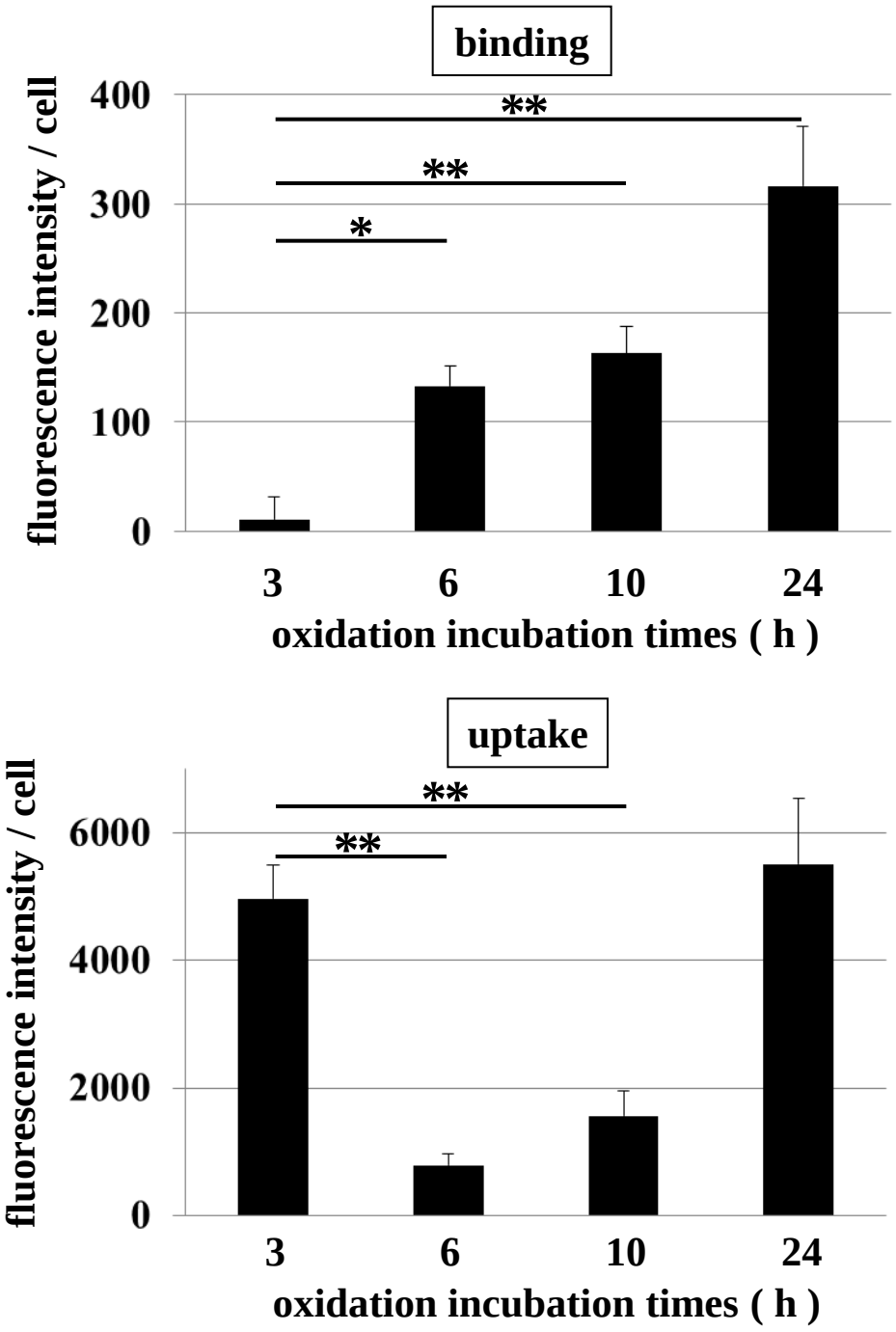

S3. Binding and uptake of OxLDL by CL-P1. CL-P1-expressing CHO cells were incubated with several OxLDL made with various oxidation incubation times (3, 6, 10 and 24 hr) on ice for 1h, followed by an endocytic reaction for 1 h at 37 °C. After incubation fixed and detected with anti-sheep anti human apolipoprotein B and Alexa Fluor 594-conjugated anti sheep IgG. Binding and uptake of OxLDL were expressed in fluorescence intensity per cell by using fluorescence microscope. Data represent means±s.e.m. (n=4 experiments). The *P* values were calculated relative to 3hr oxidation incubation time, **P*<0.05; ***P*<0.01.

Supplemental Figure 4

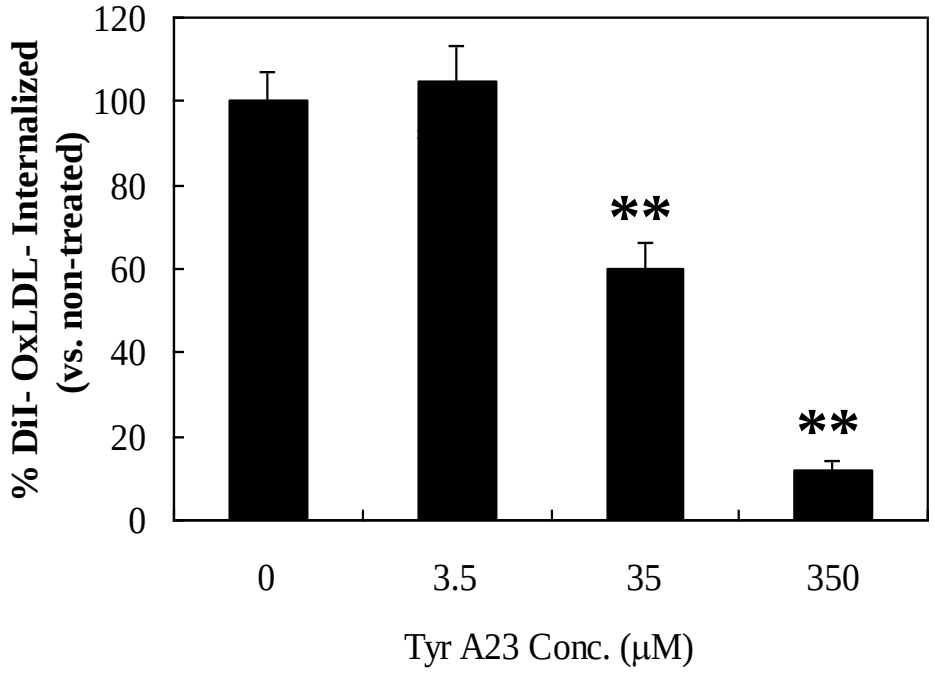

S4. Uptake of DiI-OxLDL by CL-P1-expressing cells with Tyrphostin A23. The percentage of transfected cells with internalized DiI-OxLDL was determined. Data represent means±s.e.m. (n=3 experiments). The *P* values were calculated relative to control values (nutreated), **$P<0.001$.